



# A multiobjective evolutionary algorithm using multi-ecological environment selection strategy

Shuzhi Gao, Leiyu Yang, Yimin Zhang\*

*Equipment Reliability Institute, Shenyang University of Chemical Technology, Shenyang 110142, PR China*



## ARTICLE INFO

### Article history:

Received 7 May 2021

Received in revised form 12 February 2023

Accepted 15 March 2023

Available online 3 April 2023

### Keywords:

Multi-objective optimization

Evolutionary computations

Multi-ecological environment

Convergence

Hydrodynamic sliding bearing

## ABSTRACT

For many-objective optimization problems (MaOPs), the conflict between convergence and diversity becomes more and more serious as the number of objectives increases. This paper proposes the evolutionary algorithm MeEA of multi-ecological environment selection strategy and uses this algorithm to solve MaOPs. Firstly, the objective space is divided into several different types of ecological environments. Secondly, the preference for convergence or diversity in the ecological environment is initially determined during environment selection and then the overall diversity maintenance of the population is ensured. Thirdly, the proposed algorithm is compared with five popular evolutionary algorithms on 44 multi-objective benchmark problems. Finally, it is applied to the optimization design of hydrodynamic lubrication radial sliding bearing of crane gearbox. Experimental results show that the performance of this algorithm is better than other algorithms in solving MaOPs.

© 2023 Elsevier B.V. All rights reserved.

## 1. Introduction

In practical projects, it is often necessary to optimize multiple objective problems simultaneously. However, there are irreconcilable contradictions between multiple objectives, which cannot be optimized at the same time. This problem is called multi-objective optimization problems (MOPs) [1]. In multi-objective optimization problems, due to the conflicting nature of the objectives, it is not usually possible to find a perfect solution but to obtain a set of compromise solutions to replace it, called Pareto optimal set(PS). In the past few decades, evolutionary algorithms (EAs) have shown great advantages in solving MOPs [2,3]. Therefore, a large number of multi-objective evolutionary algorithms (MOEA) have been proposed and used to solve multi-objective optimization problems, such as aerodynamic problems [4], path planning problems [5] and big data planning problems [6]. In multi-objective optimization, it is very important to define the relationship between candidate solutions. Most MOEAs distinguish the quality of candidate solutions based on the Pareto advantage method [1]. For example, NSGA-II [7] and SPEA2 (genetic algorithm II) [8] first select non-dominant solutions in the optimization process, and then use diversity maintenance mechanisms to maintain population diversity.

When more than three objectives are involved, the performance of the multi-objective optimization algorithm based on Pareto advantage decreases significantly [9,10]. When solving

two or three objective problems, the Pareto dominance-based approach can effectively distinguish the differences between candidate solutions. However, as the number of objectives increases, such Pareto-based MOEAs perform poorly, often referred to as many-objective optimization problems (MaOPs) [11]. First, as the number of objectives increases, the objective space becomes large and complex, making it difficult to explore the true pareto front(PF) with limited computing resources. This situation directly leads to an irreconcilable contradiction between convergence and diversity. Secondly, the proportion of non-dominant solutions increases dramatically as the objective dimension increases. Parato-based algorithms do not effectively distinguish candidate solutions, resulting in an inability to effectively select the appropriate solution for the next generation. This is also the fundamental reason why the solution cannot converge to true PF. So far, several methods have been proposed to solve the problems facing MaOPs, which can be roughly divided into two categories.

The first is to modify the Pareto dominance relationship. In high-dimensional objective space, the direct reason for choosing pressure loss is that the relationship between solutions cannot be distinguished. Therefore, The most effective way to solve MaOPs is to increase the selection pressure by changing the dominant relationship. The basic idea is that when the basic pareto dominance relationship is unable to distinguish a candidate solution, the convergence can be improved by increasing the selection pressure on the solution by relaxing the dominance condition or controlling the dominance angle. Examples include, dominant area control [12], subspace dominance comparison [13], preference ordering [14,15] and fuzzy Pareto dominance [16]. Although

\* Corresponding author.

E-mail address: [zhangyimin@syuct.edu.cn](mailto:zhangyimin@syuct.edu.cn) (Y. Zhang).

the difficulty in distinguishing candidate solutions can be alleviated by relaxing the individual's dominant area, further research is needed on how to select appropriate relaxation criteria [17].

The second is to use other evaluation mechanisms to increase the selection pressure on candidate solutions. The most direct way is to fully mine the effective information in the objective space. Candidate solutions seem incomparable in the objective space, but the differences between them can still be analyzed from different perspectives. On the one hand, By comparing the candidate solutions in the objective space, select the candidate solutions that have a distinct trend in an area, such as knee point-driven evolutionary algorithm (KnEA) [18], hyperplane assisted evolutionary algorithm [19], and vector angle-based evolutionary algorithm (VaEA) [12]. In addition to the detection of special individuals, using the grid concept in the decision space to detect sub-regions with special prospects to guide population evolution has also become a research direction [20]. On the other hand, some MOEAs further differentiate candidate solutions by comparing the number of differences in objective quality between candidate solutions, such as average ranking [9,21]. It is also a common method to distinguish candidate solutions by performance indicators. By calculating the contribution value of the candidate solution to the population to select the appropriate candidate solution, such as hypervolume estimation [22, 23]. But in high dimensional space, it is not easy to measure the convergence and diversity of candidate solutions by a standard. For example, HypE is less efficient than other types of algorithms. Recently, by Parato advantages with decomposition-based algorithms, it is also promising in solving MaOPs, such as MOEA/D [24] and BCE-MOEA/D [25,26]. In addition, a multi-modal evolutionary algorithm based on the dual-archive model is proposed, which is used to expand two solution spaces with different evolutionary requirements through two competition-based parallel offspring generation mechanisms, thereby improving the population evolution efficiency [27].

Although some methods can be used to increase the selection pressure of candidate solutions in high-dimensional spaces, it is difficult to maintain diversity when convergence is dominant. Similarly, when diversity is dominant, search efficiency will be reduced, and it will even lead to search stagnation [10,28,29]. Therefore, how to balance convergence and diversity is extremely important.

At present, when solving MaOPs, most MOEAs adopt the strategy of convergence first or diversity first to balance the relationship between them [30,31]. However, in the optimization process, it is difficult to consider which strategy can better solve the current MaOPs. Studies have shown that the complexity of PF is difficult to enable the algorithm to maintain good convergence while maintaining diversity. In order to improve the adaptability of the algorithm to a variety of problems, the two strategies of cascade clustering and incremental learning of reference points are interacted, and the distribution of reference points is constantly adjusted to improve the algorithm to achieve better convergence and diversity [32]. A convergence index of dimensional convergence is used to enhance the selection pressure in the environmental selection process and comprehensively evaluate individuals to select individuals [28]. However, it is difficult to use a single criterion to balance convergence and diversity [33]. To balance convergence and diversity, the fractional dominance relationship is used to improve convergence, and then the objective space decomposition is used to maintain diversity [34]. Most of the maintenance of diversity or convergence is carried out separately, but the performance of the algorithm will be reduced due to the complexity of the PF. A study shows that the convergence and diversity of candidate solutions in the objective space is a multi-objective problem [10]. MaOPs are

transformed into a dual objective problem of convergence and diversity, and then a Pareto-based method is used to solve these two objectives. Besides, the method based on ranking advantage does not choose the diversity maintenance mechanism at the beginning, but gradually increases the maintenance of diversity with the increase of iterations [9]. Therefore, when optimizing MaOPs, a good selection strategy should consider the impact of the balance between convergence and diversity on the overall performance of the algorithm.

The above research solves the many-objective optimization problems from different perspectives. However, the performance of the algorithm is still limited by the contradiction between convergence and diversity and the complexity of the real PF. According to the analysis of the real PF of the objective function, with the increase of the number of objective, the over-complexity of the objective function makes it difficult for the population to explore part of the local space, resulting in two extreme phenomena of local convergence and local sparsity [10]. Therefore, this paper proposes a multi-ecological environment selection strategy to alleviate the contradiction. By analyzing the evolutionary characteristics of individuals in the objective space, the ecological environment is established as the main body and dominates the preferences of individual selection in the environment. To demonstrate the performance of the MeEA algorithm, the proposed algorithm is compared with five popular evolutionary algorithms on 44 multi-objective benchmark instances. At the same time, the algorithm is applied to the optimal design of hydrodynamic lubrication radial sliding bearing(HLSB).

The main contributions of this work are as follows:

1. Four types of ecological environment, new environment, positive environment, crowded environment, and lazy environment are put forward.
2. An environment selection strategy is presented to alleviate the contradiction between convergence and diversity.
3. Based on the multi-ecological environment strategy and the new environment selection strategy, multi-ecological environment selection strategy evolutionary algorithm MeEA is proposed to solve MaOPs.
4. The proposed MeEA is compared with five popular algorithms on 44 benchmark problems. The experimental results demonstrate the superiority of MeEA.
5. The proposed MeEA is applied to the optimum design of HLSB in the gearbox. The experimental results show that the proposed MeEA can solve practical problems well.

The rest of this article is arranged as follows. Section 2 details the overall framework of MeEA and its implementation. In Section 3, MeEA is compared with the currently popular algorithms. In Section 4, the HLSB of the gearbox is optimized. The conclusion is given in Section 5.

## 2. Motivation

In high dimensional space, convergence and diversity balance of PF have important influence on population evolution. In order to solve this problem, most literatures improve the efficiency of population evolution by studying the dominant relationship between individuals, evaluation indexes and mixed strategies. As the number of objectives increases, the influence of inappropriate environment selection strategy on the algorithm is huge. Document [10] proposes that with the increase of the number of objective, the algorithm with good optimization effect in low-dimensional objective problems is applied to high-dimensional problems, but it brings negative influence to the algorithm. Therefore, it is very important to develop an environment selection strategy suitable for high dimensional space. At present, most

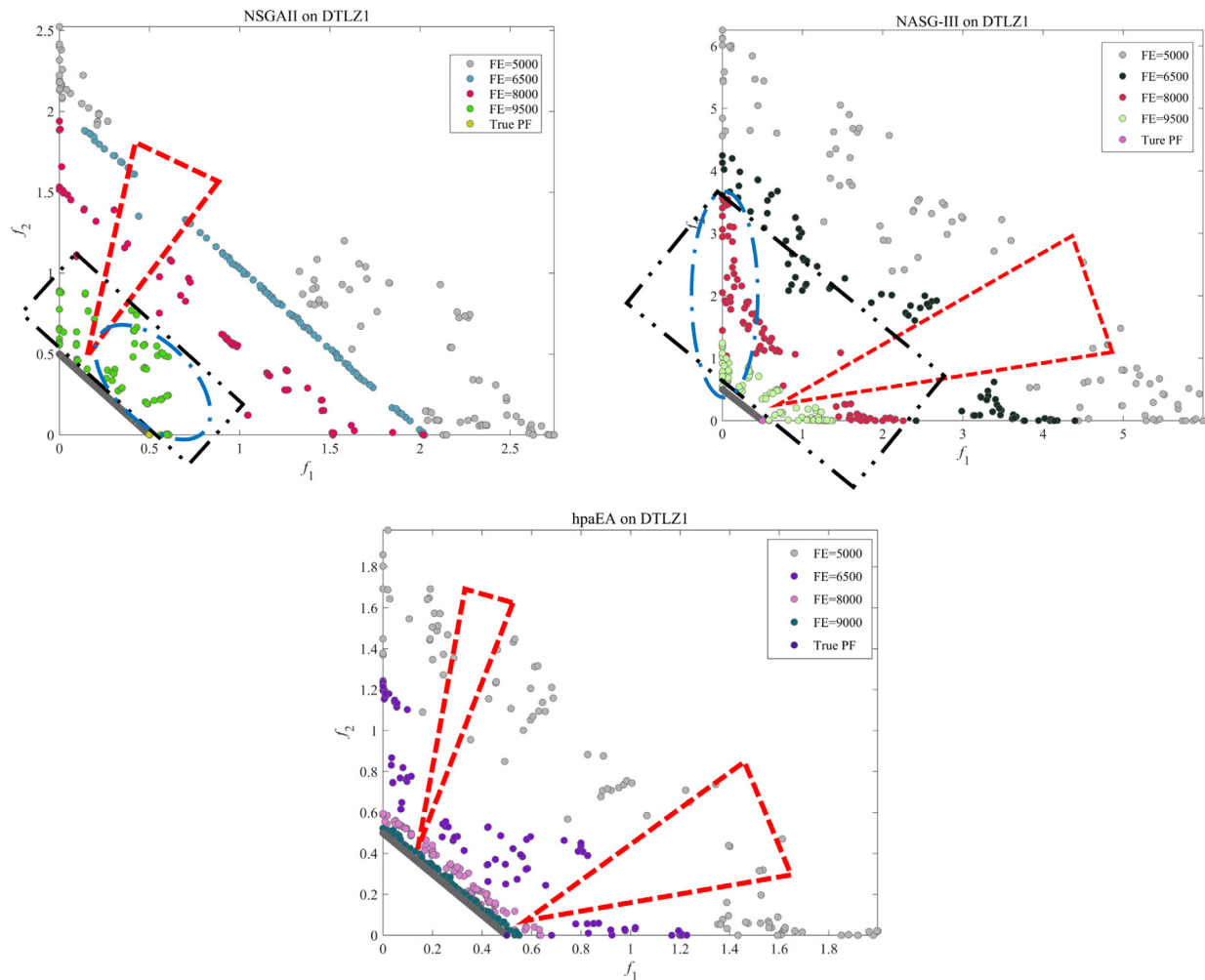


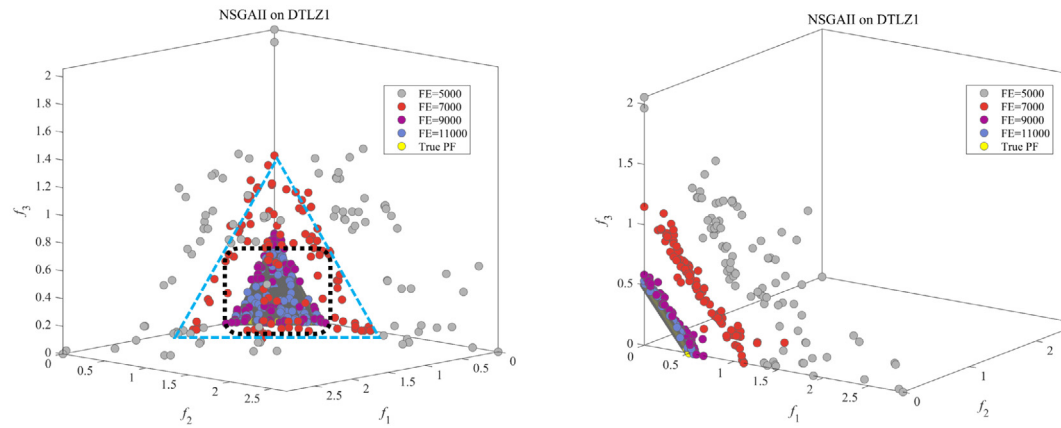
**Fig. 1.** Sampling of population distribution of NSGAII, NSGAIll and hpaEA during the iteration of 2-objective DTLZ1.

algorithms often ignore the relationship between the population distribution under the current iteration number and the real PF in the optimization of high-dimensional problems, resulting in the environmental selection strategy ignoring the influence of the real PF on the population evolution and the influence of the local space population distribution on the population evolution efficiency in the next iteration or even several iterations.

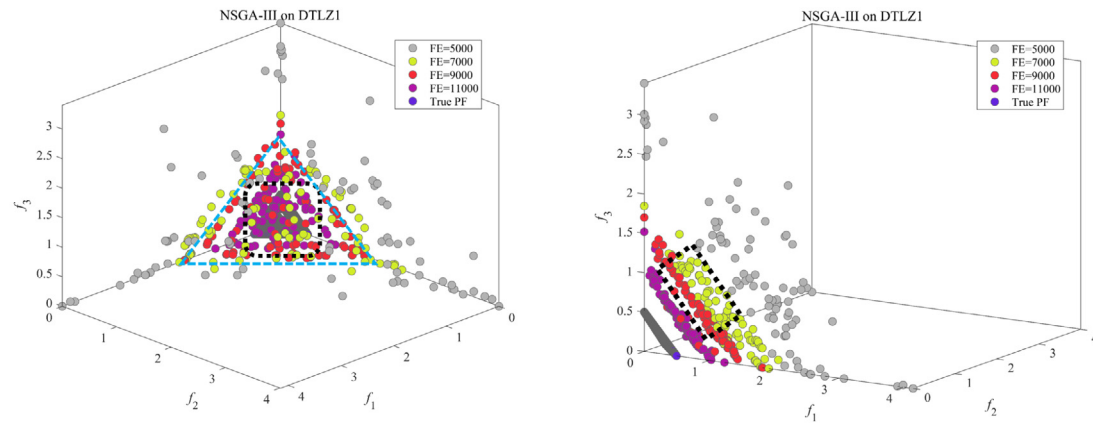
In order to better explain this phenomenon, this paper adopts the current popular algorithms NSGAII, NSGAIll and hpaEA to conduct experiments on the DTLZ1 problem of 2 and 3 objectives and describes the population distribution of these three algorithms in the optimization process. Three algorithms set the number of individuals to 100 and the number of iterations to 150. In order to prevent the initial difference between different algorithms from being too large due to the random generation of individuals during population initialization, the population distribution was sampled from the 50th iteration and the sampling results were taken for 4 times. In order to distinguish the difference of population distribution in the iterative process more clearly, the sampling interval in the DTLZ1 problem test for objective 2 and objective 3 was 15 iterations and 20 iterations, respectively.

Fig. 1 is a sample of the population distribution during the DTLZ1 problem test of NSGAII, NSGAIll, and hpaEA on objective 2. Where, the circles in different colors are the population distribution under different iterations, and FE represents the current evaluation times (iterations = FE/population number). It can be

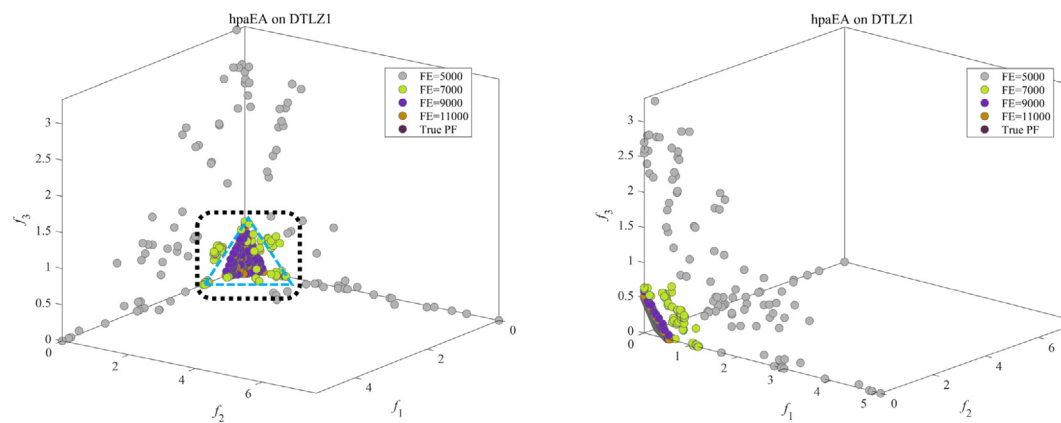
seen from the red triangle area in the figure that the number of individuals in this area is sparse after 50 iterations. After sampling the population distribution in subsequent iterations, the individual diversity in this region was still not improved, resulting in the lack of diversity in this region. In the above three algorithms, the situation is still not improved after the later iteration due to the lack of diversity in the early part of the space. In the black box area in the figure, the three algorithms converge to the local area with a large number of individuals, while the individual distribution in some objective space is sparse. Such population distribution did not improve the efficiency of evolution. On the contrary, too many individuals retained in one region would inevitably lead to the loss of diversity and convergence in other evolutionary regions, which would be detrimental to the overall evolution of the population. In the optimization process of NSGAIll for DTLZ1 problem, the black circle in the 65th iteration and the red circle in the 80th iteration was compared in the blue ellipse region. Some positions of the red circle and the black circle were transitional adjacent, indicating that the population evolution efficiency was very low and even stagnated after 15 iterations in this region. The occurrence of this situation in the middle of iteration is not conducive to the population approaching the real PF, and the individual retention in this region is relatively more than that in other regions, which will also affect the diversity and convergence of other evolutionary regions. On the other hand, if a population has evolved significantly in that region, it indicates that individuals have a greater desire to explore in that space



(a) Front view of population distribution of NSGAII on DTLZ1 (b) Profile of population distribution of NSGAII on DTLZ1



(c) Front view of population distribution of NSGAIII on DTLZ1 (d) Profile of NSGAIII population distribution on DTLZ1



(e) Front view of population distribution of hpaEA on DTLZ1

(f) Profile of hpaEA distribution on DTLZ1

**Fig. 2.** Sampling of population distribution of NSGAII, NSGAIII and hpaEA during the iteration of 2-objective DTLZ1.

than in other regions. Selecting suitable environmental selection strategy in this region may have a good effect on the evolutionary efficiency of the population.

**Fig. 2** shows the population distribution sampling of NSGAII, NSGAIII and hpaEA in the DTLZ1 problem test of objective 3. Fig.(a), (c) and (e) are the front view of NSGAII, NSGAIII and

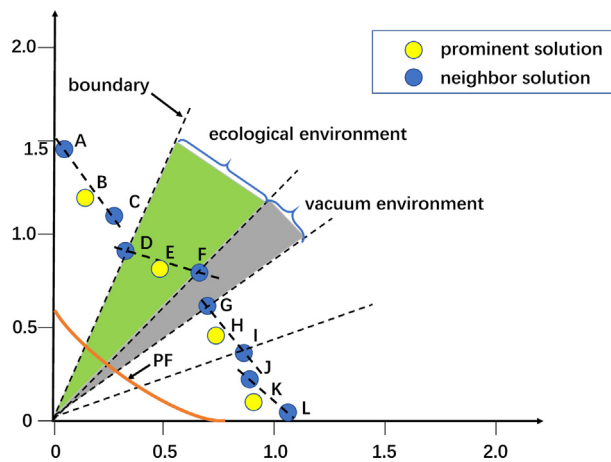


**Fig. 3.** Illustration of the ecological environment established with a  $P_s$ .

hpaEA population distribution respectively, and Fig.(b), (d) and (f) are the side view of corresponding population distribution respectively. In the figure, the real PF of DTZL1 presents a triangle, but the central part of the population distribution of the three algorithms under the number of 50–90 iterations is relatively sparse, and the individual concentration converges to the edge of the triangle, as shown in the blue box in the figure. Similarly, excessive convergence in one region leads to insufficient diversity in other regions. In the three-dimensional space, the black box in Fig. (d) also shows the close proximity of the population distribution of the two adjacent generations, so it can be seen that the population evolution efficiency is low or even stagnant in local areas of the two generations. Therefore, the transition of retained individuals in this area is not beneficial to the population as a whole. It can be seen from the result of Fig. (d) when the number of iterations is 110 that the population distribution still has a certain distance from the real PF.

It can be seen from the DTLZ1 problem test of different algorithms on 2 and 3 objectives that different environment selection strategies have similar problems in the optimization process, such as individual sparsity and crowding in local space and low evolutionary efficiency or even stagnation. However, these environmental selection strategies do not solve these problems well and thus perpetuate them. The complexity of the objective function makes it difficult for the population to explore part of the local space, resulting in two extreme phenomena of local convergence and local sparsity. Therefore, this paper abstracts the problems of sparseness, crowding, low evolutionary efficiency or even stagnation in the population distribution into the ecological environment characteristics of the objective space. According to the classification of the ecological environment, and the appropriate environmental selection strategy is formulated.

### 3. The proposed method

In high-dimensional space, due to the complexity of the objective space, it is difficult for the population to explore part of the local space in the evolution process, resulting in local convergence and local sparsity of the population, making it difficult for the population to get close to the real PF. Therefore, this paper abstracts the problems of sparsity, crowding, low evolutionary efficiency and even stagnation in population distribution into the ecological environment characteristics of the objective space.

### 3.1. Main procedure of MeEA

As shown in Algorithm 1, Lines 1 to 3 mainly carry out the initialization of parameters: (1) initialize the population  $P$ ; (2) the current function evaluation number  $FEs$ ; (3) initialize the prominent solution  $P_s$  and its number  $k$ . The rest is the main loop of the proposed algorithm MeEA (lines 4–13). In each generation, the algorithm performs the following three steps: (1) the generation of mating pools; (2) the generation of offspring; (3) environmental selection. In this article, the method of generating the mating pool is to liberate all the  $P_s$  into the mating pool. First, calculate the number of prominent solutions  $k$  (line 5). Then, randomly select  $N - k$  individuals in the current population and put them into the mating pool, even if the prominent solution index may be repeated in the population (line 6). Finally, put all  $P_s$  into the mating pool (line 7). The proposed MeEA algorithm uses simulated binary crossover and polynomial mutation to generate individual offspring (line 8). In the environmental selection of the population, the strategy of selecting individuals according to the ecological environment of the objective space is combined.

---

#### Algorithm 1 A General Framework of MeEA

---

**Input:** MOP; population size  $N$ ; maximum function evaluations(MFEs); objective dimension  $M$ ;  
**Output:** The final population  $P$ ;

- 1: Initialize a population  $P$  randomly;
- 2: Record  $FEs \leftarrow N$ ;
- 3: Initialize prominent solutions as  $P_s \leftarrow \emptyset$ , and its number is  $k$ ;
- 4: **while**  $FEs < MFEs$  **do**
- 5:      $k \leftarrow |P_s|$ ;
- 6:      $I \leftarrow$  Randomly generate  $N - k$  integers;
- 7:      $I \leftarrow I \cup \{1, 2, \dots, k\}$ ;
- 8:      $P' \leftarrow$  GeneratieOffsprings ( $P(I)$ );
- 9:      $Q \leftarrow P \cup P'$
- 10:    prominent solutions of the previous generation  $P_{sp}$ :  $P_{sp} \leftarrow P_s$
- 11:     $FEs = FEs + N$ ;
- 12:     $[P, P_s] \leftarrow$  popSelectionStrategy ( $Q, P_{sp}, M, N$ );
- 13: **end while**

---

### 3.2. Multi-ecological environment selection strategy

Different problems have different shapes of the PF, and therefore also determine the complexity of the objective space environment. Therefore, this paper classifies the objective space by analyzing the change of population distribution during the continuous evolution process. Local sparse, local dense, low evolutionary efficiency and high evolutionary efficiency objective space were defined as new ecological environment, crowded ecological environment, lazy ecological environment and active ecological environment respectively. To avoid various problems when dividing the ecological environment of the objective space, such as a large number of calculations in high-dimensional space of the grid division and the contradiction between adjacent grids. In this study, firstly, the solution with obvious trend is regarded as the center of local ecological environment, which is called prominent solution  $P_s$  [19]. Secondly, find the  $M$  neighbors of the prominent solution as neighbors. Finally, considering the complexity of the objective space environment, the ecological environment is classified.

The establishment of the ecological environment is illustrated in Fig. 3. In the two-dimensional space, the prominent solution  $P_s$  is identified by judging whether the individual is below the hyperplane formed by its adjacent solutions. In Fig. 3, the hyperplane of the prominent solution is composed of line structures

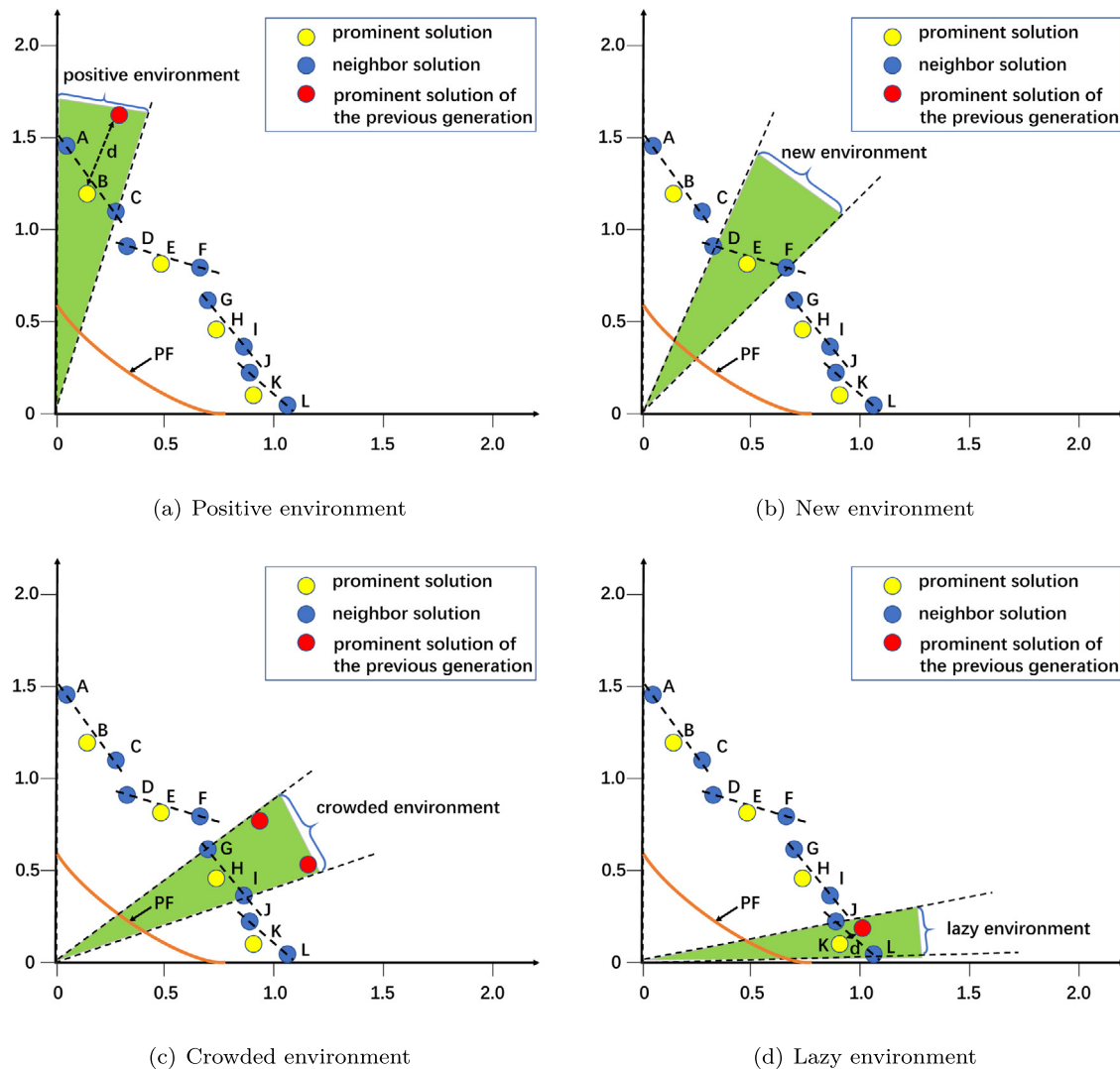


**Fig. 4.** Multi-type ecological environment. (a) Positive environment. (b) New environment. (c) Crowded environment. (d) Lazy environment.

associated with adjacent solutions  $D$  and  $F$  (dotted line in two-dimensional space).  $E$  is regarded as the center of ecological environment. The cosine similarity between neighbors  $D$  and  $F$  to  $E$  is regarded as the boundary of the ecological environment. The green area in the picture represents the ecological environment centered on the prominent solution  $E$ . It should be noted that the distance between  $D$  and  $F$  to  $E$  is not necessarily equal. The multiple ecological environments are not seamlessly connected. There may be a vacuum environment between the ecological environment, such as the gray area in the figure.

The multi-ecological environment strategy is to classify the objective space by comparing the relationship between the  $P_s$  of two adjacent generations. Fig. 4 vividly shows the different ecological environments. In Fig. 4(a), if the previous generation  $P_s$  (redpoint) appears in the ecological environment centered on point  $B$ , and the Euclidean distance  $d$  between them is greater than the average Euclidean distance between  $A$  and  $C$  to  $B$ , then the ecological environment is defined as a positive environment. The characteristic of a positive ecological environment is that the objective space can produce effective individuals more likely. Relatively speaking, invalid individuals mean that the evolution of individuals in this space is in a relatively stagnant state. Similarly, if  $d$  is less than the average Euclidean distance from  $A$  and  $C$  to  $B$ , the environment is defined as lazy environment. The characteristic of a lazy environment is that the individual evolution

in the objective space is in a relatively stagnant state, as shown in Fig. 4(d). In Fig. 4(b), if there is no previous generation of  $P_s$  in the ecological environment centered on prominent solution  $E$ , the ecological environment is defined as a new environment. The characteristics of the new environment are new space areas that may be explored, which are of great value to the maintenance of diversity. In Fig. 4(c), if more than two (the case involving two previous generation of solutions) previous generation  $P_s$  are found in the area with  $H$  as the ecological environment, the environment is defined as a crowded environment. The feature of the crowded environment is that the two  $P_s$  are very close to each other in the objective space due to the overcrowding of individuals.

Algorithm 2 introduces the classification of the ecological environment of the objective space. First, find  $P_s$  in the non-dominated solution  $L_1$  (line 1). Then calculate the basic attributes of the ecological environment where  $P_s$  is located. Its basic attributes include the size of the ecological environment and the neighbors contained in the ecological environment (lines 2–8). The detailed steps of establishing the ecological environment are as follows: (1) Count the number of  $P_s$  and the number of remaining non-dominated solutions  $k$  (lines 1–2); (2) Initialize the type of ecological environment  $C_z$ . There are four types of ecological environment, namely, the new environment  $C_1$ , the

active environment  $C_2$ , the crowded environment  $C_3$  and the lazy environment  $C_4$ ; (3) Calculate the cosine similarity  $c_k^j$  between  $P_s$  and other non-dominated solutions; (4) Compare the cosine similarity between  $P_s$  and other individuals, and use the nearest individuals of  $M$  as the neighbors of  $P_s$  and record it as  $C^k$ ; (5) The average cosine similarity between the neighbors and  $P_s$  as the space size of the  $k$ th ecological environment  $c_k^{mean}$ . The ecological environment is classified according to the Euclidean distance between two adjacent generations of  $P_s$  (lines 2–8). The detailed steps of classification are as follows: (1) Find out the prominent solution  $P_{sp}^k$  of the previous generation belonging to the  $k$ th ecological environment, the number of which is  $l$  (line 10); (2) If  $l \geq 2$ , then the ecological environment is defined as crowded (line 12); (3) If  $l = 1$ , it is necessary to judge adjacent the Euclidean distance between two generations of  $P_s$ ; If the distance is greater than the average Euclidean distance from the neighbor to  $P_s$ , the ecological environment is defined as a positive type. On the contrary, it is defined as lazy (Lines 13–20); (4) If  $l = 0$ , define the ecological environment as a new environment (Line 22). By classifying all the spaces where  $P_s$  is located, a number of  $k$  of different sizes and different types of ecological environments are obtained in the objective space.

#### Algorithm 2 Function classification( $L_1, P_{sp}, M$ )

**Input:** Non-dominated solution  $L_1$ ; prominent solutions of the previous generation  $P_{sp}$ ; objective dimension  $M$ ;

**Output:** Category of ecological environment  $C_z$ ; ecological environment size  $c_k^{mean}$ ; neighbor  $G_k$ ; prominent solution  $P_s$ ;

```

1: Search prominent solution  $P_s$ ;
2:  $L'_1 \leftarrow L_1 \setminus P_s$ ;
3:  $k \leftarrow |P_s|; j \leftarrow |L'_1|$ ;
4: Initialize ecological environment as:  $C_z, z = 1, 2, 3, 4$ ;
5: Calculate the cosine similarity between  $P_s$  and other non-
   dominant individuals:  $c_k^j \leftarrow \frac{P_s^k l_1^j}{\|P_s^k\| \cdot \|l_1^j\|}$ 
6: Sort  $c_k^j$  in ascending order;
7: The neighbors of the  $P_s^k$  are individual satisfying  $c_k^j \leq c_k^M$ , expressed as  $G_k$ ;
8: The size of the environment ecological of the  $P_s^k$  as:  $c_k^{mean} \leftarrow \text{mean}(\sum_{i=1}^M c_k^M)$ ; the ecological environment is  $C^k$ ;
9: for  $i = 1 \rightarrow k$  do
10:    $l \leftarrow |P_{sp} \cap C^k|; P_{sp}^k \leftarrow P_{sp} \cap C^k$ ;
11:   if  $l \geq 2$  then
12:      $C_3 \leftarrow$  Define the ecological environment of the  $P_s^k$  as a
        crowded ecological;
13:   else if  $l=1$  then
14:      $d \leftarrow$  Calculate the Euclidean distance between  $P_{sp}^k$  and
         $P_s^k$ ,
15:      $d_k^{mean} \leftarrow$  Calculate the average Euclidean distance
        between  $P_s$  and its neighbors;
16:     if  $d \geq d_k^{mean}$  then
17:        $C_2 \leftarrow$  Define the ecological environment of the  $P_s^k$ 
        as a positive ecological;
18:     else
19:        $C_4 \leftarrow$  Define the ecological environment of the  $P_s^k$ 
        as a lazy ecological;
20:     end if
21:   else
22:      $C_1 \leftarrow$  Define the ecological environment of the  $P_s^k$  as a
        new ecological;
23:   end if
24: end for
```

### 3.3. Environmental selection strategy

MaOPs optimization requires not only increasing the pressure on individual selection but also maintaining the diversity of the population. When the number of non-dominant solutions in a population is larger than that in a population, it is not feasible to use only the Pareto advantage to compare the advantages and disadvantages between individuals. To solve this problem, the first consideration in environmental selection is to select individuals in the ecological environment. Different ecological environment characteristics are considered and individuals are maintained in different ways into the next generation. Then, other non-dominant solutions are chosen based on the cosine similarity between individuals to maintain the diversity of the PF in the objective space. Unlike the method of considering the diversity of the whole space or the convergence of a single individual, the proposed environment selection method first chooses the offspring in terms of the local objective space. When the number of non-dominant solutions in the population is less than that in the population, non-dominant solutions are given priority to entering the next generation, and some dominant solutions should be selected to maintain diversity.

Algorithm 3 introduces the proposed environment selection strategy. Initialize the number of prominent solutions  $k$  (line 1). Divide the population  $Q$  into different levels by the method of non-dominated sorting ( $L_1, L_2, \dots$ ) (Line 2). Two different offspring selection methods are adopted according to the number of non-dominated solutions  $L_1$ . One situation is that when the number of non-dominated solutions  $L_1$  is greater than the number of population  $N$ , a strategy of combining multiple ecological environments is proposed to select offspring. First, the objective space is divided into four types by the ecological environment classification strategy  $C_z$  (line 4). Then, the convergence of neighbors in each ecological environment is calculated  $c(G_k)$  (line 5). Finally, reserve the neighbors in the ecological environment (lines 6–15). Different ecological environments have different preferences for convergence or diversity. The detailed steps of neighbor reservation are as follows: (1) If the environment type is new environment  $C_1$  or active environment  $C_2$ , i.e.  $z = 1$  or  $z = 2$ , the same selection strategy is adopted (line 7); calculate the environmental quantity  $L_c$  of this ecological type (line 8). This type of ecological environment is selected in turn for neighbors (lines 9–10). Three neighbors with the minimum convergence index value in the ecological environment are selected as the auxiliary solution  $A_s$  (line 10); (2) If the environment type is lazy  $C_4$ , that is,  $z = 4$ , then the neighbor with the least convergence index value in the ecological environment is selected (line 13). It is important to note that neighbors are not preserved in crowded environments. Different ecological environments adopt different levels of retention strategies. The more neighbor individuals selected in the ecological environment, the greater the preference for convergence. But it does not mean that the diversity of the entire PF can be ignored. The diversity of the population is maintained by the function `MaintainDiversity()` (line 17). Another situation is when the number of non-dominated solutions  $L_1$  is less than the number of population  $N$ . First consider keeping the non-dominated solutions  $L_1$ . Then, select part of the dominant solution among the candidate solutions  $R$  to maintain diversity (lines 19–25). Calculate the cosine similarity between the  $k$ th non-dominated solution and the  $j$ th candidate solution as  $c_k^j$  (line 21). Treat each non-dominated solution as the center of an ecological environment. Take the cosine similarity between the non-dominated solution and its nearest individual as the size of the ecological environment  $c_k^{mean}$  (line 22). The auxiliary solution assignment value is empty (line 23). The function `MaintainDiversity()` is used to balance diversity and convergence (line 24).

**Algorithm 3** Function popSelectionStrategy( $Q, P_{sp}, M, N$ )

**Input:** Combined population Q; population size N; prominent solutions of the previous generation  $P_{sp}$ ; objective dimension M; population size N;

**Output:** The final population P; prominent solutions  $P_s$

- 1: Initialize the number of prominent solutions as:  $k \leftarrow 0$ ;
- 2:  $[L_1, L_2, \dots] \leftarrow$  Non-dominated-sort (Q);
- 3: **if**  $|L_1| > N$  **then**
- 4:    $[C_z, c_k^{mean}, G_k, P_s] \leftarrow$  classification( $L_1, P_{sp}, M$ );
- 5:   Calculate the convergence of neighbors:  $c(G_k) \leftarrow \text{agg}(f_1(\mathbf{x}), \dots, f_M(\mathbf{x}))$ ;
- 6:   **for**  $z=1 \rightarrow 4$  **do**
- 7:     **if**  $z = 1 \parallel z = 2$  **then**
- 8:        $L_c \leftarrow |P_s \cap C_z|$ ;
- 9:       **for**  $i=1 \rightarrow L_c$  **do**
- 10:          $A_s \leftarrow$  Choose the three neighbor solutions with the smallest  $c(G_i)$  from  $G_i$  as auxiliary solutions;
- 11:       **end for**
- 12:     **else if**  $z = 4$  **then**
- 13:        $A_s \leftarrow$  Choose the one neighbor solutions with the smallest  $c(G_i)$  from  $G_i$  as auxiliary solutions;
- 14:     **end if**
- 15:   **end for**
- 16:   Construct the candidate solution set as:  $R \leftarrow Q \setminus [P_s, A_s]$ ;
- 17:    $P = \text{MaintainDiversity}(P_s, A_s, R, c_k^{mean}, N)$ ;
- 18: **else**
- 19:    $R \leftarrow R \setminus L_1$ ;
- 20:    $k \leftarrow |L_1|; j \leftarrow |R|$ ;
- 21:   Calculate the cosine similarity between  $L_1$  and R:  $c_k^j \leftarrow \frac{L_1^k \cdot R}{\|L_1\| \cdot \|R\|}$ ;
- 22:   Calculate the size of the environment ecological of the non-dominated solution as:  $c_k^{mean} \leftarrow \min(c_k^j)$ ;
- 23:    $A_s \leftarrow \emptyset$
- 24:    $P = \text{MaintainDiversity}(L_1, A_s, R, c_k^{mean}, N)$
- 25: **end if**

Algorithm 4 introduces the detailed flow of the function MaintainDiversity(). The diversity maintenance mechanism adopted when the number of non-dominated solutions is larger or smaller than the population size is very similar. The main content is around the selected individual S and the candidate solution R. First, generate N uniformly distributed m-dimensional unit vectors V (line 1). Then, calculate the cosine similarity between S and V (line 4). If  $V^i$  belongs to the jth ecological environment of S, eliminate  $V^i$ . In other words, during diversity maintenance, individuals near the unit vector will not be considered (lines 5–7). Finally, select some candidate solutions to maintain population diversity (lines 10–17). Calculate the cosine similarity between the candidate solution and the unit vector  $\cos \theta(R, i)$  (line 14). Calculate the cosine similarity between the nearest individuals  $v^i \min \cos \theta_{j,i}$  (line 15). Select the jth individual to enter S until the sum of  $A_s$  and S meets the population requirement N, and stop diversity maintenance. Combine the retained individuals into a new population P (line 18).

**4. Performance evaluation**

In this section, the experimental design to verify the performance of MeEA is introduced. The algorithms for comparison are: (1) BiGE [10]; (2) SPEAR [35]; (3) KnEA [18]; (4) hpaEA [19].

The comparison algorithm and the proposed algorithm are coded in MATLAB 2018a and embedded into the evolutionary

**Algorithm 4** MaintainDiversity ( $S, A_s, R, c_k^{mean}, N$ )

**Input:** Selected solution S; candidate solution R; non-dominated solution  $L_1$ ; ecological environment size  $c_k^{mean}$ ; population size N;

**Output:** The final population P;

- 1: Generate N uniformly distributed m-dimensional unit vectors as  $V \leftarrow \{\mathbf{v}^1, \mathbf{v}^2, \dots, \mathbf{v}^N\}$ ;
- 2: **for**  $j = 1 \rightarrow |S|$  **do**
- 3:   **for**  $i = 1 \rightarrow N$  **do**
- 4:      $\cos \theta_{j,i} = \frac{S_j \cdot v^i}{\|S_j\| \cdot \|v^i\|}$ ;
- 5:     **if**  $\cos \theta_{j,i} < c_k^{mean}$  **then**
- 6:        $V \leftarrow V \setminus v^i$ ;
- 7:     **end if**
- 8:   **end for**
- 9: **end for**
- 10: **for**  $i = 1 \rightarrow |V|$  **do**
- 11:   **if**  $|S| + |A_s| > N$  **then**
- 12:     break;
- 13:   **end if**
- 14:    $\cos \theta_{R,i} = \frac{R \cdot v^i}{\|R\| \cdot \|v^i\|}$ ;
- 15:    $\min \cos \theta_{j,i} \leftarrow \min(\cos \theta_{R,i})$
- 16:    $S \leftarrow S \cup R_j$ ;
- 17: **end for**
- 18:  $P \leftarrow S \cup A_s$ ;

**Table 1**

Characteristics of the benchmark problems.

Problem	n	Characteristics
DTLZ1	$M + 4$	Linear, Multimodal
DTLZ2	$M + 9$	Concave
DTLZ3	$M + 9$	Concave, MultiModal
DTLZ4	$M + 4$	Concave, Biased
DTLZ5	$M + 9$	Concave, Degenerate
DTLZ6	$M + 9$	Concave, Degenerate, Biased
DTLZ7	$M + 19$	Mixed, Disconnected, Multimodal, Scaled

multi-objective optimization platform PlatEMO [36]. All experiments were run on a PC with 8.0 GB RAM, two Intel (R) Core (TM) CPUs i5-8300 h, and 64-bit window 10 operating system.

**4.1. Experimental settings****4.1.1. Benchmark problems**

In this study, the benchmark DTLZ [37] is used to compare the performance of six algorithms. In benchmark DTLZ, the real PF of different benchmark problems have different characteristics. The Characteristics performance of these characteristics is summarized in Table 1. Besides, the scaled DTLZ1-DTLZ2 (SDTLZ1-SDTLZ2), convex DTLZ1(C1\_DTLZ1) and convex DTLZ3 (C1\_DTLZ3) [38] have also been added to the test. This paper selects 3, 5, 8, and 10 objective benchmark problems.

**4.1.2. Performance metric and population size**

To measure the performance of different algorithms on benchmark problems, inverted generational distance(IGD) [39] and hypervolume (HV) [40], which are widely used, are used to calculate the performance of the algorithms.

The HV represents the volume of the hypercube enclosed by the individual in the solution set and the reference point in the objective space . The HV index can simultaneously express the convergence and diversity of the PF. The higher the HV value, the better the performance of the algorithm and vice versa. According to the reference point in literature [41],  $\mathbf{r}_{1 \times m} = \{r, r, \dots, r\}$  is

**Table 2**

Setting of population size.

Number of objectives	H	MeEA
3	12	92
5	6	212
8	3	156
10	3	276

recommended to be set to  $r = 1 + 1/H$ , Where  $H$  needs to meet  $C_{m-1}^{H+m-1} \leq N < C_{m-1}^{H+m}$ . Using the parameter setting method in literature [19], the population size and the setting of parameter  $H$  are shown in Table 2. For a fair comparison, the population sizes of NSGA-III, SPEAR, BiGE, KnEA, hpaEA and MeEA are consistent on different benchmark problems.

IGD expresses the convergence performance and distribution performance of the algorithm by calculating the minimum distance sum between the point on the true PF surface and the individual set obtained by the algorithm. IGD is calculated as follows:

$$\text{IGD}(P^*, P) = \frac{\sum_{v \in P^*} D_{\min}(v, P)}{|P^*|} \quad (1)$$

where  $P^*$  is expressed as a uniformly distributed set of points collected in true PF;  $P$  is represented as a population;  $D_{\min}(v, P)$  is expressed as the minimum Euclidean distance from point  $v$  to all individuals in  $P$ . The smaller the value of IGD, the better the performance of the algorithm, and vice versa.

#### 4.1.3. Termination condition

The maximum function evaluation number (MFE) is used as the termination condition of the algorithm. Set the MFE of the six algorithms to 100 000. Each algorithm is independently run 30 times on each benchmark problems and records the average and standard deviation of the IGD value. Besides, Wilcoxon's rank-sum test was used to calculate the difference between the performance indicators of the algorithm, and the null hypothesis was rejected at the 0.05 level of significance.

## 4.2. Experimental results and analysis

### 4.2.1. Analysis of performance indicators

Tables 3 and 4 are the statistical results of the IGD value and HV value of the six algorithms on the benchmark DTLZ, respectively. The mean and standard deviation (in parentheses) of statistics after 30 iterations are recorded. To better reflect the difference in results, the best results for each benchmark example are bold. At the same time, the Wilcoxon rank-sum test with alpha = 0.05 is used to verify the significant difference between the proposed MeEA and other algorithms in the performance index results. The symbols +, -, ≈ indicate significantly superior, inferior, and similar to the proposed MeEA, respectively.

As shown in Table 3. In 11 three-objective benchmark problems, the proposed MeEA has no obvious advantages compared with other algorithms. Among them, the performance of hpaEA on the DTLZ1-4 and DTLZ7 benchmark problems is better than other algorithms. But it shows better performance in other benchmark problems. For the 5-objective benchmark problems, the performance of the proposed MeEA is better than the other 5 algorithms in 8 out of 11 test cases. Among them, the DTLZ1-3, C1\_DTLZ, and SDTLZ series of test examples are significantly better than the first five algorithms. For 8 and 10 dimension test cases, the proposed algorithm also shows better performance. MeEA performed better than other algorithms in 14 out of 22 test cases. In general, the performance index IGD of the proposed algorithm MeEA has advantages in 26 of the 44 test cases.

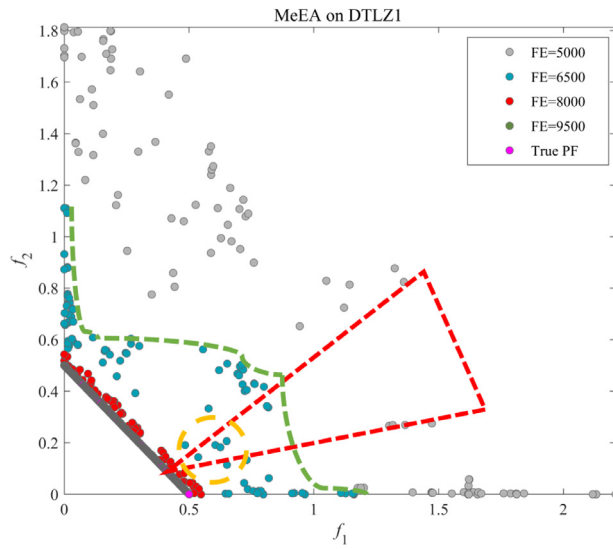
By comparing the statistical mean and standard deviation of performance indicators of the six algorithms in Tables 3 and 4 after 30 iterations, it can be seen that the mean and standard deviation of performance indicators of the proposed algorithm MeEA are smaller, so it has better robustness. The results of Wilcoxon rank sum test show that the proposed algorithm is superior to other algorithms.

Table 4 shows the HV values of the proposed MeEA and the compared algorithm on the DTLZ1-7 benchmark problems. The experimental results have again verified the superiority of MeEA. In more detail, MeEA is significantly better than the previous five algorithms on 4, 8, 11, 12, and 16 benchmark problems. The comparative advantages of MeEA algorithms can be attributed to the following facts. The proposed MeEA uses a multi-ecological environment strategy to divide the objective space into several different types of subspaces. Among them, different ecological environments have different effects on individual evolution. First, in the selection of the offspring of a population, the impact of the current objective space's ecological environment on the evolution of offspring is considered, which can better guide individuals toward the true PF. Second, a uniformly distributed reference vector is used to select the remaining individuals to ensure overall diversity of the population.

### 4.2.2. Analysis of multi-ecological environment strategy and environment selection strategy

In order to solve the problems of local sparsity, local congestion and low efficiency of local evolution in the objective space, four kinds of ecological environment and suitable environmental selection strategy are proposed. In order to illustrate the proposed multi-ecological environment strategy and environment selection strategy and its impact on the algorithm, Figs. 5 and 6 show the population distribution of the proposed algorithm under the same experimental settings as Figs. 1 and 2 respectively. As can be seen from the red triangle in Fig. 5, when the number of iterations is 50, the problem of sparse individuals in local space appears in the population distribution. Different from other algorithms, the proposed algorithm defines the objective space as a new ecological environment in subsequent iterations, and proposes to reserve as many individuals as possible in the environment to improve the ability to explore the objective space in the process of environment selection. In subsequent iterations, the problem faded away, with the yellow circles indicating improvement. In order to improve the evolutionary efficiency of population, the regions with low evolutionary efficiency and high evolutionary efficiency were defined as lazy environment and active environment respectively. In the process of environmental selection, two different environmental selection strategies are proposed to prevent local convergence and promote individuals' ability to explore the objective space. The dotted green line in Fig. 5 is the boundary line of population distribution when the number of iterations is 65. It can be seen from the figure that the low efficiency of population evolution has been significantly improved. In addition, compared with other algorithms, the proposed algorithm can approach the real PF more quickly from the population distribution interval under different iterations. In order to prevent the over-aggregation of individuals in some regions from leading to the loss of overall diversity, the objective space was defined as a crowded environment, and the strategy of reducing individual retention in this region was formulated. As can be seen from Fig. 3, the phenomenon of transition convergence in local space has been improved to some extent.

In order to illustrate the practicability of the proposed multi-ecological environment and environment selection strategy in high-dimensional objective space, Fig. 6 is a sample front and side diagram of MeEA population distribution in the DTLZ1 problem



**Fig. 5.** Sampling of MeEA population distribution during DTLZ1 iteration of 2 objectives.

test of 3 objectives. The black box in Fig. 6(a) indicates that local sparsity appears in the center of the population distribution when the number of iterations is 50. It can be seen from the samples of the following three population distributions that the proposed algorithm has a good effect on solving the problem of triangle edge convergence and center sparsity. As can be seen from the population distribution intervals under different iterations in Fig. 6(b), the convergence speed of the proposed algorithm is significantly improved compared with other algorithms.

**Table 3**

Comparison of IGD between six algorithms of benchmark DTLZ1-7, C1\_DTLZ1, C1\_DTLZ3, SDTLZ1 and SDTLZ2 and 3, 5, 8, and 10 objectives.

Problem	M	NSGAII	SPEAR	BiGE	KnEA	hpEA	MeEA
DTLZ1	3	2.0567e-2 (1.22e-5) -	3.2893e-2 (2.59e-2) -	4.3829e-2 (3.04e-2) -	6.5756e-2 (3.82e-2) -	<b>1.9819e-2 (9.54e-5) +</b>	2.0154e-2 (2.74e-4)
DTLZ1	5	5.2831e-2 (1.79e-4) -	8.1118e-2 (2.64e-2) -	1.0713e-1 (4.44e-2) -	1.6502e-1 (6.66e-2) -	5.0615e-2 (2.43e-4) -	<b>4.7953e-2 (5.42e-4)</b>
DTLZ1	8	1.1804e-1 (4.27e-2) -	1.5687e-1 (5.09e-2) -	2.5967e-1 (5.85e-2) -	7.7100e-1 (9.02e-1) -	1.3300e-1 (6.32e-2) -	<b>9.3165e-2 (2.30e-3)</b>
DTLZ1	10	1.4834e-1 (5.34e-2) -	3.8861e-1 (1.87e-1) -	7.3885e-1 (3.89e-1) -	4.5346e+0 (2.90e+0) -	5.1615e-1 (2.62e-1) -	<b>9.7073e-2 (4.34e-3)</b>
DTLZ2	3	5.4464e-2 (5.57e-7) -	5.7071e-2 (1.23e-3) -	8.3896e-2 (4.71e-3) -	6.9535e-2 (3.31e-3) -	5.3428e-2 (3.94e-4) ≈	<b>5.3248e-2 (9.44e-4)</b>
DTLZ2	5	1.6513e-1 (1.75e-5) -	1.6818e-1 (1.01e-1) -	2.0719e-1 (4.11e-3) -	1.7739e-1 (2.98e-3) -	1.5939e-1 (6.47e-4) -	<b>1.5886e-1 (1.52e-3)</b>
DTLZ2	8	3.2206e-1 (3.23e-2) +	<b>3.1881e-1 (1.49e-3) +</b>	4.0229e-1 (5.09e-3) -	3.8230e-1 (5.86e-3) -	3.4137e-1 (2.05e-2) +	3.5992e-1 (1.95e-2)
DTLZ2	10	4.4596e-1 (3.74e-2) ≈	<b>4.2869e-1 (1.76e-3) +</b>	4.5005e-1 (5.06e-2) ≈	4.4305e-1 (3.03e-2) +	4.5040e-1 (2.50e-2) ≈	4.4646e-1 (1.88e-2)
DTLZ3	3	5.4658e-2 (1.68e-4) +	2.0767e-1 (8.39e-2) -	1.1598e-1 (2.98e-2) -	1.0775e-1 (2.82e-2) -	<b>5.4169e-2 (3.18e-4) +</b>	5.5567e-2 (7.76e-4)
DTLZ3	5	1.7002e-1 (6.05e-3) -	7.8573e-1 (4.88e-1) -	5.0877e-1 (1.95e-1) -	4.2454e-1 (1.47e-1) -	1.7341e-1 (1.81e-2) -	<b>1.6227e-1 (1.24e-3)</b>
DTLZ3	8	1.3578e+0 (1.58e+0) -	1.0529e+0 (4.58e+0) -	1.5095e+1 (5.33e+0) -	9.5433e+1 (3.14e+1) -	8.0041e+1 (2.68e+0) -	3.4193e-1 (5.39e-3)
DTLZ3	10	2.6290e+0 (2.70e+0) -	5.5612e+1 (2.12e+1) -	2.7747e+1 (1.05e+1) -	3.7277e+2 (1.37e+2) -	5.5506e+1 (1.75e+1) -	<b>9.6425e-1 (8.29e-1)</b>
DTLZ4	3	1.5190e-1 (1.98e-1) +	<b>5.7444e-2 (1.08e-3) +</b>	1.1134e-1 (1.58e-1) +	6.9043e-2 (2.64e-3) +	3.0346e-1 (2.49e-1) +	4.0544e-1 (2.58e-1)
DTLZ4	5	<b>1.6516e-1 (3.65e-5) ≈</b>	1.6860e-1 (1.36e-3) ≈	2.0891e-1 (5.44e-3) ≈	1.7601e-1 (3.94e-3) ≈	2.3817e-1 (1.28e-1) +	2.6883e-1 (1.34e-1)
DTLZ4	8	3.8533e-1 (1.01e-1) -	<b>3.2200e-1 (1.47e-3) +</b>	3.9810e-1 (5.25e-3) ≈	3.7347e-1 (5.94e-3) ≈	3.7110e-1 (5.11e-2) ≈	3.8457e-1 (5.03e-2)
DTLZ4	10	4.2929e-1 (1.98e-2) -	4.5376e-1 (5.16e-3) -	6.3669e-1 (2.93e-2) -	4.3431e-1 (4.94e-3) -	4.5054e-1 (1.29e-2) -	<b>4.1469e-1 (4.60e-3)</b>
DTLZ5	3	1.2531e-2 (1.52e-3) -	3.1743e-2 (3.97e-3) -	1.7046e-2 (4.21e-3) -	1.0688e-2 (2.18e-3) -	<b>5.3149e-3 (1.43e-4) +</b>	5.7796e-3 (2.79e-4)
DTLZ5	5	8.2985e-2 (2.34e-2) ≈	1.8340e-1 (3.13e-2) -	9.4514e-2 (1.51e-2) -	1.5407e-1 (3.34e-2) -	9.5653e-2 (1.92e-2) -	<b>7.1119e-2 (1.35e-2)</b>
DTLZ5	8	2.4489e-1 (7.24e-2) -	5.1320e-1 (1.35e-1) -	2.0051e-1 (4.53e-2) ≈	2.8434e-1 (6.44e-2) -	3.2309e-1 (7.27e-2) -	1.8863e-1 (3.52e-2)
DTLZ5	10	3.2432e-1 (9.89e-2) -	6.5815e-1 (1.25e-1) -	3.2085e-1 (7.61e-2) -	3.3671e-1 (7.59e-2) -	3.6353e-1 (7.59e-2) -	<b>1.7915e-1 (3.61e-2)</b>
DTLZ6	3	2.0177e-2 (2.65e-3) -	3.7606e-2 (5.28e-3) -	7.0498e-1 (4.71e-2) -	2.0745e-2 (1.33e-2) -	4.9857e-3 (1.35e-4) ≈	<b>4.9590e-3 (1.09e-4)</b>
DTLZ6	5	<b>1.6677e-1 (3.65e-5) +</b>	2.9074e-1 (9.05e-2) ≈	6.7233e-1 (7.99e-2) -	2.7051e-1 (8.09e-2) ≈	2.4357e-1 (1.19e-1) +	3.1543e-1 (1.22e-1)
DTLZ6	8	<b>5.4781e-1 (3.37e-1) ≈</b>	9.6762e-1 (2.72e-1) -	6.8026e-1 (5.64e-2) -	7.4082e-1 (2.71e-1) -	1.6487e+0 (5.35e-1) -	5.8714e-1 (1.95e-1)
DTLZ6	10	6.7377e-1 (3.02e-1) ≈	2.3275e+0 (5.81e-1) -	6.6647e-1 (6.65e-2) ≈	1.6435e+0 (4.15e-1) -	2.8240e+0 (4.88e-1) -	<b>6.0634e-1 (1.48e-1)</b>
DTLZ7	3	8.7151e-2 (5.58e-2) +	9.5499e-2 (2.33e-3) +	1.9028e-1 (2.04e-1) -	1.1207e-1 (1.50e-1) -	<b>8.6173e-2 (6.42e-2) +</b>	9.7204e-2 (5.97e-2)
DTLZ7	5	2.8454e-1 (1.06e-2) -	3.5536e-1 (6.13e-3) -	3.8959e-1 (1.24e-1) -	<b>2.4219e-1 (6.53e-3) +</b>	2.8707e-1 (7.66e-2) -	2.6275e-1 (3.75e-2)
DTLZ7	8	7.8954e-1 (3.18e-2) -	1.1853e+0 (3.71e-2) -	1.9538e+0 (3.37e-1) -	<b>6.4008e-1 (3.05e-2) -</b>	4.7356e-1 (1.46e-2) -	7.0900e-1 (2.44e-2)
DTLZ7	10	1.1312e+0 (8.54e-2) -	2.0825e+0 (5.28e-2) -	3.3000e+0 (4.45e-1) -	<b>8.6781e-1 (1.19e-2) +</b>	1.1551e+0 (1.14e-1) -	8.8639e-1 (4.73e-2)
C1_DTLZ1	3	<b>2.0477e-2 (6.40e-5) +</b>	4.1264e-2 (3.37e-2) -	4.4067e-2 (2.32e-2) -	2.1585e-2 (2.22e-4) -	2.4502e-2 (8.01e-4) -	2.1294e-2 (5.34e-4)
C1_DTLZ1	5	5.1783e-2 (4.91e-4) -	8.9198e-2 (1.89e-2) -	1.2725e-1 (5.45e-2) -	6.2240e-2 (9.55e-4) -	5.3802e-2 (6.31e-4) -	<b>4.7992e-2 (7.00e-4)</b>
C1_DTLZ1	8	9.7108e-2 (7.83e-3) -	1.8309e-1 (2.72e-2) -	2.7818e-1 (6.16e-2) -	1.0232e-1 (1.49e-3) -	1.8744e-1 (4.38e-2) -	<b>9.5760e-2 (3.19e-3)</b>
C1_DTLZ1	10	<b>1.0834e-1 (3.51e-3) +</b>	4.7992e-1 (1.13e-1) -	4.1777e-1 (4.89e-2) -	1.1028e-1 (1.06e-3) +	4.8708e-1 (1.34e-1) -	1.2790e-1 (1.80e-2)
C1_DTLZ3	3	4.6096e+0 (3.96e+0) -	1.6491e-1 (5.34e-2) -	1.0161e-1 (2.15e-2) -	<b>5.3922e-2 (3.14e-4) +</b>	6.9582e+0 (2.74e+0) -	5.5109e-2 (7.19e-4)
C1_DTLZ3	5	1.0029e+1 (3.55e+0) -	4.3494e-1 (4.88e-2) -	3.7920e-1 (6.40e-2) -	9.5087e+0 (4.30e+0) -	<b>1.6227e-1 (6.92e-3)</b>	
C1_DTLZ3	8	1.0366e+1 (3.48e+0) -	1.9761e+0 (1.96e+0) -	2.5951e+0 (1.94e+0) -	1.4226e+1 (2.86e+0) -	1.5067e+0 (6.12e-1) -	<b>3.4529e-1 (2.02e-2)</b>
C1_DTLZ3	10	1.3941e+1 (1.96e+0) -	1.4398e+1 (2.04e+0) -	9.2293e+0 (8.81e+0) -	3.6950e+1 (1.19e+1) -	1.4213e+1 (2.06e+0) -	<b>1.1870e+0 (2.85e-1)</b>
SDTLZ1	3	5.1507e-2 (3.17e-5) -	8.4359e-2 (6.54e-2) -	1.1428e-1 (6.39e-2) -	4.9362e-2 (2.83e-4) -	1.1732e-1 (7.49e-2) -	<b>4.9024e-2 (6.49e-4)</b>
SDTLZ1	5	3.8245e-1 (2.76e-3) -	4.3504e-1 (7.41e-2) -	5.8030e-1 (1.67e-1) -	3.3996e-1 (5.96e-3) -	8.0892e-1 (2.53e-1) -	<b>2.6046e-1 (4.39e-3)</b>
SDTLZ1	8	3.5038e+0 (5.73e-1) -	4.1622e+0 (8.57e-1) -	6.6527e+0 (2.07e+0) -	5.5275e+0 (1.47e+0) -	3.1237e+0 (7.52e-1) -	<b>2.5112e+0 (1.33e-1)</b>
SDTLZ1	10	1.2161e+1 (3.55e+0) -	1.5779e+1 (5.33e+0) -	3.3342e+1 (6.84e+0) -	1.0757e+2 (5.41e+1) -	1.3128e+1 (3.49e+0) -	<b>7.8368e+0 (4.42e-1)</b>
SDTLZ2	3	1.2988e-1 (3.21e-6) -	1.3440e-1 (2.28e-3) -	1.8881e-1 (1.08e-2) -	1.2698e-1 (9.47e-4) -	1.6012e-1 (5.80e-3) -	<b>1.2308e-1 (3.25e-3)</b>
SDTLZ2	5	9.8512e-1 (6.99e-4) -	9.9921e-1 (4.68e-3) -	1.1272e+0 (2.63e-2) -	9.2418e-1 (9.26e-3) -	1.0679e+0 (2.56e-2) -	<b>8.5151e-1 (1.71e-2)</b>
SDTLZ2	8	1.1338e+1 (2.22e+0) -	1.0857e+1 (7.14e-2) -	1.0626e+1 (6.48e-1) -	1.3231e+1 (4.57e-1) -	8.8283e+0 (3.02e-1) ≈	<b>8.7377e+0 (4.17e-1)</b>
SDTLZ2	10	3.9508e+1 (1.38e+0) -	4.3216e+1 (1.21e+0) -	3.6109e+1 (1.77e+0) -	4.7554e+1 (2.13e+0) -	<b>3.2843e+1 (1.69e+0) ≈</b>	3.3028e+1 (1.76e+0)
+/ - ≈		7/33/4	5/37/2	1/38/5	7/34/3	8/30/6	

**Table 4**

Comparison of HV between six algorithms of benchmark DTLZ1-7 and 3, 5, 8, and 10 objectives.

Problem	M	NSGAIII	SPEAR	BiGE	KnEA	hpaEA	MeEA
DTLZ1	3	8.4159e-1 (1.64e-4) ≈	8.1258e-1 (5.99e-2) -	7.8836e-1 (6.04e-2) -	7.1666e-1 (7.73e-2) -	<b>8.4313e-1 (2.54e-4)</b> +	8.4129e-1 (5.77e-4)
DTLZ1	5	9.7957e-1 (3.03e-4) +	9.5883e-1 (2.29e-2) -	9.1288e-1 (9.85e-2) -	7.0832e-1 (1.59e-1) -	<b>9.8099e-1 (3.27e-4)</b> +	9.7508e-1 (1.50e-3)
DTLZ1	8	<b>9.8046e-1 (5.43e-2)</b> +	9.1854e-1 (1.41e-1) -	7.6852e-1 (1.66e-1) -	4.6236e-1 (4.10e-1) -	9.4017e-1 (1.37e-1) -	9.7697e-1 (6.09e-3)
DTLZ1	10	9.7005e-1 (9.00e-2) -	3.7214e-1 (2.72e-1) -	1.4735e-1 (2.31e-1) -	0.0000e+0 (0.00e+0) -	3.1563e-1 (3.68e-1) -	<b>9.9461e-1 (2.13e-3)</b>
DTLZ2	3	5.5962e-1 (3.18e-6) +	5.5681e-1 (1.83e-3) ≈	5.3542e-1 (4.88e-3) -	5.4105e-1 (3.43e-3) -	<b>5.6048e-1 (3.81e-4)</b> +	5.5627e-1 (1.24e-3)
DTLZ2	5	8.1228e-1 (3.91e-4) +	8.0982e-1 (1.05e-3) +	7.8890e-1 (2.94e-3) -	7.9156e-1 (3.61e-3) -	<b>8.1608e-1 (9.49e-4)</b> +	8.0697e-1 (1.56e-3)
DTLZ2	8	<b>9.2067e-1 (1.52e-2)</b> +	9.1896e-1 (1.04e-3) +	8.9628e-1 (5.61e-3) +	8.8514e-1 (7.15e-3) ≈	9.1063e-1 (1.60e-2) +	8.8767e-1 (1.52e-2)
DTLZ2	10	<b>9.6182e-1 (1.23e-2)</b> +	9.5896e-1 (1.39e-3) +	9.5993e-1 (1.92e-3) +	9.5522e-1 (1.89e-2) +	9.3866e-1 (1.49e-2) +	9.2701e-1 (1.40e-2)
DTLZ3	3	<b>5.5631e-1 (2.17e-3)</b> +	4.3082e-1 (6.42e-2) -	4.9240e-1 (3.58e-2) -	4.9850e-1 (3.11e-2) -	<b>5.5610e-1 (2.65e-3)</b> +	5.5401e-1 (2.78e-3)
DTLZ3	5	7.8856e-1 (1.50e-2) -	2.6860e-1 (2.01e-1) -	4.7269e-1 (1.58e-1) -	4.9734e-1 (1.36e-1) -	7.8825e-1 (2.75e-2) -	<b>8.0209e-1 (3.22e-3)</b>
DTLZ3	8	5.0218e-1 (4.08e-1) -	0.0000e+0 (0.00e+0) -	0.0000e+0 (0.00e+0) -	0.0000e+0 (0.00e+0) -	0.0000e+0 (0.00e+0) -	<b>9.0577e-1 (6.21e-3)</b>
DTLZ3	10	1.2979e-1 (2.32e-1) -	0.0000e+0 (0.00e+0) -	0.0000e+0 (0.00e+0) -	0.0000e+0 (0.00e+0) -	0.0000e+0 (0.00e+0) -	<b>4.8673e-1 (3.64e-1)</b>
DTLZ4	3	5.1547e-1 (8.96e-2) +	<b>5.5586e-1 (1.49e-3)</b> +	5.2271e-1 (8.16e-2) +	5.4177e-1 (3.11e-3) +	4.4010e-1 (1.19e-1) +	3.8652e-1 (1.28e-1)
DTLZ4	5	<b>8.1184e-1 (4.63e-4)</b> +	8.0818e-1 (1.17e-3) ≈	7.9058e-1 (3.42e-3) ≈	7.9633e-1 (3.07e-3) ≈	7.7880e-1 (5.97e-2) +	7.6416e-1 (6.12e-2)
DTLZ4	8	8.9754e-1 (3.83e-2) +	<b>9.1576e-1 (1.12e-3)</b> ≈	9.0693e-1 (3.38e-3) ≈	9.0231e-1 (5.84e-2) ≈	8.9994e-1 (2.45e-2) ≈	8.9468e-1 (3.45e-2)
DTLZ4	10	9.6728e-1 (6.91e-3) -	9.5555e-1 (2.98e-3) -	7.7840e-1 (5.79e-2) -	9.5813e-1 (2.74e-3) -	9.4392e-1 (4.91e-3) -	<b>9.7071e-1 (1.44e-3)</b>
DTLZ5	3	1.9395e-1 (1.32e-3) -	1.8285e-1 (3.03e-3) -	1.9257e-1 (1.97e-3) -	1.9238e-1 (2.33e-3) -	<b>1.9936e-1 (1.34e-4)</b> +	1.9902e-1 (3.15e-4)
DTLZ5	5	<b>1.1505e-1 (4.00e-3)</b> +	2.7011e-2 (1.76e-2) -	1.1453e-1 (3.63e-3) +	8.2610e-2 (1.85e-2) ≈	7.1761e-2 (2.28e-2) ≈	8.3117e-2 (1.89e-2)
DTLZ5	8	<b>9.3802e-2 (2.56e-3)</b> +	1.4557e-3 (5.01e-3) -	9.1370e-2 (7.45e-4) +	7.3804e-2 (1.78e-2) +	6.2705e-3 (1.06e-2) -	1.3182e-2 (2.09e-2)
DTLZ5	10	8.4545e-2 (5.55e-3) +	2.9217e-4 (1.53e-3) -	<b>9.0580e-2 (3.54e-4)</b> +	3.4362e-2 (3.02e-2) +	2.2428e-3 (5.26e-3) -	9.1533e-3 (1.28e-2)
DTLZ6	3	1.9054e-1 (1.87e-3) -	1.8151e-1 (3.04e-3) -	9.2743e-2 (3.10e-3) -	1.8591e-1 (1.05e-2) -	1.9981e-1 (5.19e-5) ≈	<b>1.9982e-1 (1.519e-5)</b>
DTLZ6	5	<b>9.8346e-2 (1.80e-2)</b> +	1.2747e-2 (1.79e-2) ≈	9.4157e-2 (4.43e-3) +	9.2967e-2 (5.97e-3) +	6.26857e-2 (2.64e-2) +	1.6978e-2 (2.93e-2)
DTLZ6	8	6.9725e-2 (3.91e-2) +	2.9160e-3 (1.35e-2) ≈	<b>9.2606e-2 (1.81e-3)</b> +	9.0956e-3 (2.78e-2) ≈	1.0116e-4 (5.18e-4) ≈	7.7213e-4 (2.70e-3)
DTLZ6	10	1.8158e-2 (3.47e-2) ≈	0.0000e+0 (0.00e+0) -	<b>9.2513e-2 (1.34e-3)</b> +	0.0000e+0 (0.00e+0) -	0.0000e+0 (0.00e+0) -	3.0304e-3 (1.66e-2)
DTLZ7	3	2.6905e-1 (6.81e-3) ≈	2.6873e-1 (1.26e-3) -	2.5842e-1 (2.13e-2) ≈	2.7190e-1 (1.60e-2) +	2.6500e-1 (9.09e-3) -	<b>2.6978e-1 (6.89e-3)</b>
DTLZ7	5	2.5765e-1 (3.20e-3) -	2.4914e-1 (2.19e-3) -	2.6257e-1 (8.55e-3) -	2.6158e-1 (2.91e-3) -	2.6306e-1 (5.64e-3) -	<b>2.6977e-1 (3.59e-3)</b>
DTLZ7	8	2.0002e-1 (3.14e-3) -	1.6137e-1 (1.44e-2) -	<b>2.1153e-1 (6.16e-3)</b> +	1.3765e-1 (2.77e-2) -	1.9384e-1 (3.10e-3) -	2.0861e-1 (3.71e-3)
DTLZ7	10	1.6791e-1 (5.34e-3) -	1.3991e-1 (1.21e-2) -	<b>1.8673e-1 (9.72e-3)</b> +	8.2786e-2 (3.17e-2) -	1.5904e-1 (6.65e-3) -	1.8098e-1 (4.91e-3)
+/ - / ≈		15/10/3	4/19/5	11/14/3	6/17/5	11/13/4	

the proposed algorithm MeEA. From Fig. 7(a) and (f), it can be seen that the aggregate values in the objective dimensions of the algorithms NSGA-III and MeEA converge between 0 and 0.6. Some solutions for algorithm NSGA-III overlap in the objective space and some dimensions do not exist. Therefore, the performance of the algorithm NSGA-III in maintaining diversity is poor. It is obvious from Fig. 7(e) that hpaEA can maintain a certain diversity, but its PF has poor convergence. Comparing the six algorithms from the perspective of diversity and convergence, it can be seen that the proposed algorithm MeEA has better performance in balancing diversity and convergence.

For DTLZ3 with 8 objectives. Except for the proposed algorithm MeEA, the PF of other algorithms has not converged between 0 and 1. Therefore, it can be further concluded that the proposed algorithm MeEA can further approximate true PF while maintaining diversity. MeEA's strategy in different ecological environments is to adjust local convergence and diversity before maintaining global convergence and diversity. This is helpful to alleviate the contradiction between the two and keep the population close to the true PF. To further verify the performance of the six algorithms. Fig. 9 shows the evolutionary trajectory of the IGD values of NSGA-III, SPEAR, BiGE, KnEA, hpaEA, and MeEA on DTLZ1, DTLZ3, and SDTLZ1 of the 8 objectives. Among them, the change in the IGD value is the result of taking the logarithm of it. It can be seen from 9(a) that the convergence speed of NSGA-III is faster than other algorithms, followed by the proposed MeEA. From the 34 000 evaluations of NSGA-III indicated in Fig. 9, its convergence speed became flat, and before 45 000 evaluations, the proposed MeEA still maintained the same convergence speed. The proposed MeEA still maintains the same convergence speed until 45,000 evaluations. In the process of convergence of the algorithms KnEA and BiGE, there are even varying degrees of distance from the true PF. As can be seen from Fig. 9(b) and (c), in terms of convergence speed, the convergence speed of the proposed MeEA is significantly better than the other five algorithms. Fig. 10 shows the evolution trajectory of IGD values of six algorithms on DTLZ1, DTLZ3, and SDTLZ1 of five objectives. In terms of the convergence speed of IGD, the convergence speed of MeEA still has obvious advantages compared with other algorithms. In the iterative process, the IGD values of the six algorithms are decreasing. However, some algorithms, such as NSGA-III, SPEAR, and KnEA, have some rebound in the IGD values of benchmark DTLZ1. This situation is also reflected in other

benchmark problems. Compared with the other five algorithms, the IGD value of MeEA keeps a downward trend. The final results show that the proposed MeEA has obvious advantages over other algorithms. The results prove the effectiveness of MeEA again.

Four ecological environments were proposed, and corresponding environmental selection strategies were proposed to effectively solve the problems of local space difficult to be searched, local convergence and low efficiency of population evolution due to the complexity of real PF of objective space. However, because the proposed environmental selection strategy is not entirely suitable for different ecological environments, it may be difficult to improve the efficiency of population evolution in some local objective Spaces. Therefore, it is necessary to continue to study the adaptability of each ecological environment to environmental selection strategy and improve the optimization ability of adaptive algorithm.

#### 4.2.3. Algorithm complexity analysis

In this summary, a time complexity analysis of MeEA is provided. Based on pseudo code in Algorithm 1, time complexity is determined by 5–12 rows of entry loops. When calculating the following time complexity, the influence of decision variables and objectives is generally ignored because they are much smaller than the size of population and external file N. In line 8, the complexity of the process for generating the offspring population is O(3N). In line 10, the complexity of finding the salient solution is O(N). In line 12, ecosystem classification in Algorithm 2, environment selection in Algorithms 3 and 4 diversity maintenance are performed, with complexity of O(N), O(N) and O(N<sup>2</sup>), respectively. Based on the above analysis, MeEA's time complexity is O(6N + N<sup>2</sup>).

Table 5 shows the average computing time for NSGAIII, SPEAR, BiGE, KnEA, hpaEA, and MeEA to solve DTLZ test problems for all five objectives. The average time of each problem is obtained from 30 separate runs, and the time unit is seconds. It can be seen from the table that the proposed algorithm performs only faster than SPEAR. In addition, compared with BiGE, KnEA and hpaEA, the average execution speed of the proposed algorithm is similar. Therefore, this shows that the proposed algorithm MeEA has a certain disadvantage in computing time compared with other algorithms. This is mainly because dividing the objective space into multiple ecological environments will increase the computing time of the algorithm.

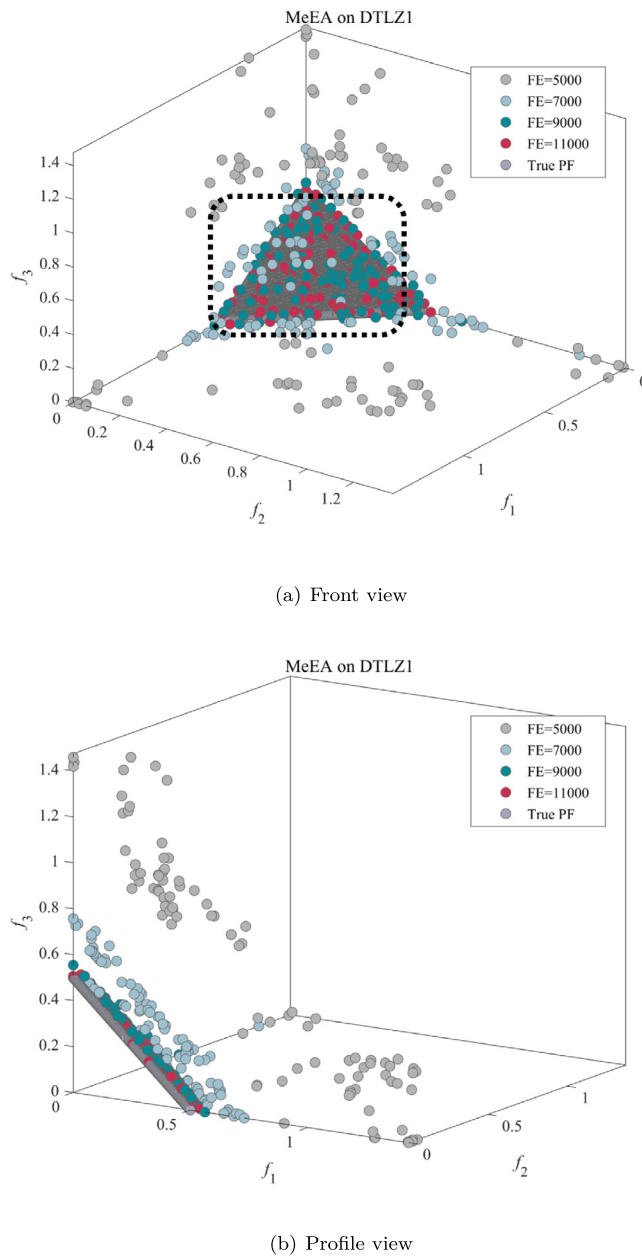


**Fig. 6.** Sampling of MeEA population distribution during DTLZ1 iteration of 3 objectives.

**Table 5**

The average computing time for NSGAIII, SPEAR, BiGE, KnEA, hpaEA.

Problem	NSGAIII	SPEAR	BiGE	KnEA	hpaEA	MeEA
DTLZ1	2.76	18.76	4.58	6.71	9.79	12.62
DTLZ2	2.93	18.61	5.08	9.85	12.2	16.53
DTLZ3	2.82	18.56	4.35	5.68	7.72	8.48
DTLZ4	3.01	18.36	5.4	10.01	11.29	14.62
DTLZ5	4.02	18.35	5.88	9.3	14.94	14.11
DTLZ6	3.86	18.6	5.47	8.49	12.13	13.59
DTLZ7	4.19	18.9	5.16	9.47	11.92	13.53

## 5. Optimum design of HLRSB for gearbox

Optimization problems in the real world usually involve multiple objectives, and these objectives should be optimized at the same time. The traditional mathematical methods cannot solve these problems effectively. Therefore, the MeEA algorithm is applied to the optimization design of the hydrodynamic lubrication

radial sliding bearing of the gearbox of the crane to improve the bearing performance. The model diagram of the HLRSB is shown in Fig. 11.

### 5.1. Problem formulation of HLRSB design

HLRSBs are mainly used for special operating conditions, such as extremely high speed, precise support requirements, extremely high loads, heavy impact, split type, etc. It seems to have a simple external geometry, but different shape parameter settings may have different effects on bearing performance. The optimization of HLRSB consists of three parts: design parameters, objective functions, and constraints [42,43].

#### 5.1.1. Design variable

The main design parameters of HLRSB are as follows:

$$X = [x_1, x_2, x_3]^T = [B/d, \psi, \eta]^T \quad (2)$$

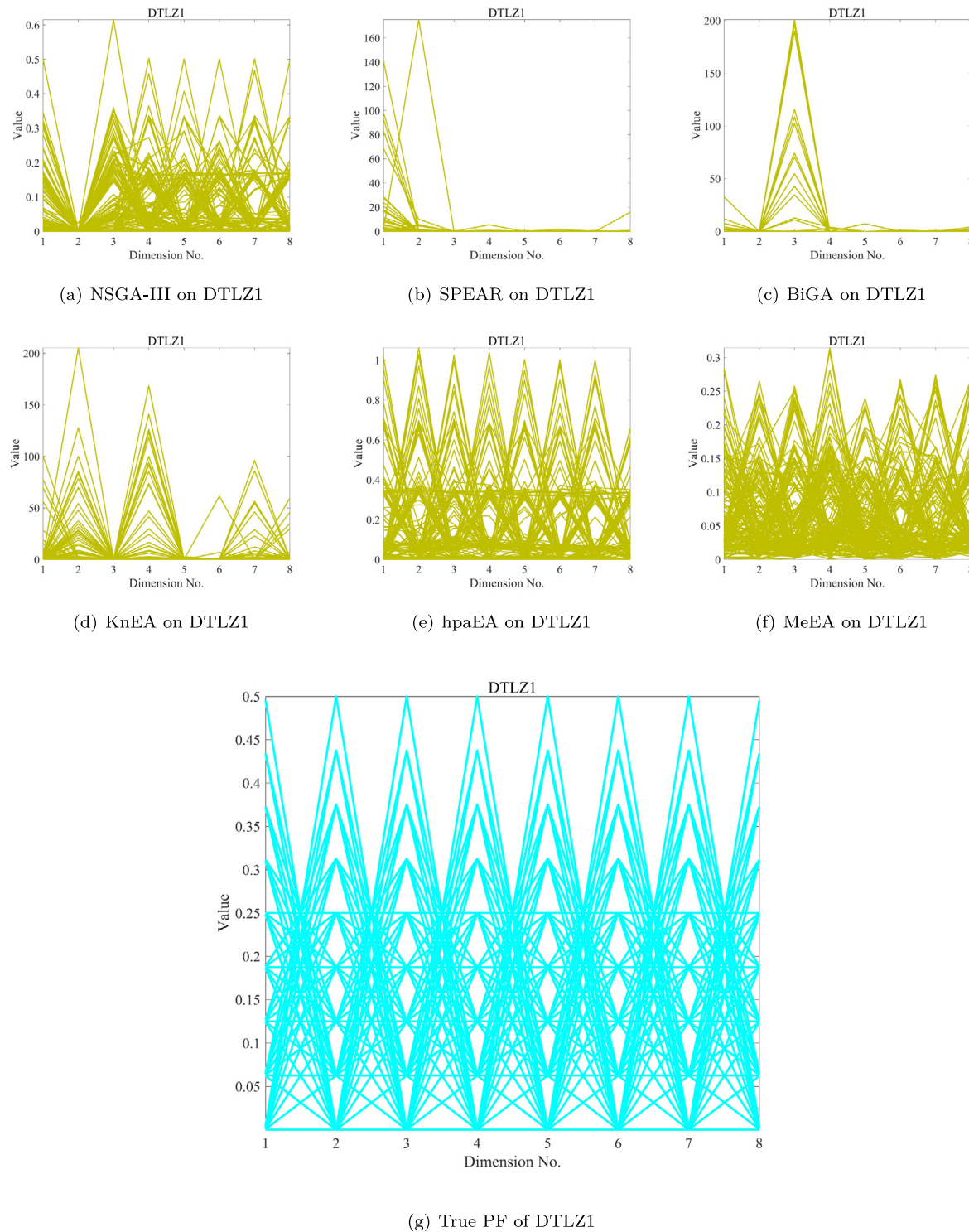


**Fig. 7.** The output populations of the six algorithms on 8-objective DTLZ1. (a) NSGA-III on DTLZ1. (b) SPEAR on DTLZ1. (c) BiGA on DTLZ1. (d) KnEA on DTLZ1. (e) hpaEA on DTLZ1. (f) MeEA on DTLZ1. (g) True PF of DTLZ1.

where  $B/d$  is width-to-diameter ratio, and  $B$  and  $d$  represent the width and diameter of the bearings respectively;  $\psi$  is relative clearance;  $\eta$  is dynamic viscosity of lubricants (see Appendix for the nomenclature).

#### 5.1.2. Objective function

The HLRSB has three important performance indexes, namely, liquid friction coefficient, heat generation, and carrying capacity coefficient. To obtain the best bearing performance, the objective

is to minimize heat generation, minimize friction coefficient and maximize load capacity. The objective functions are as follows:

$$\min f_1(X) = f = \frac{\pi \eta \omega}{p \psi} + 0.55 \psi \xi \quad (3)$$

$$\min f_2(\mathbf{X}) = p v = \frac{F v}{x_1 d^2} \quad (4)$$

$$\max f_3(X) = C_p = \frac{P \psi^2}{\eta \omega} \quad (5)$$

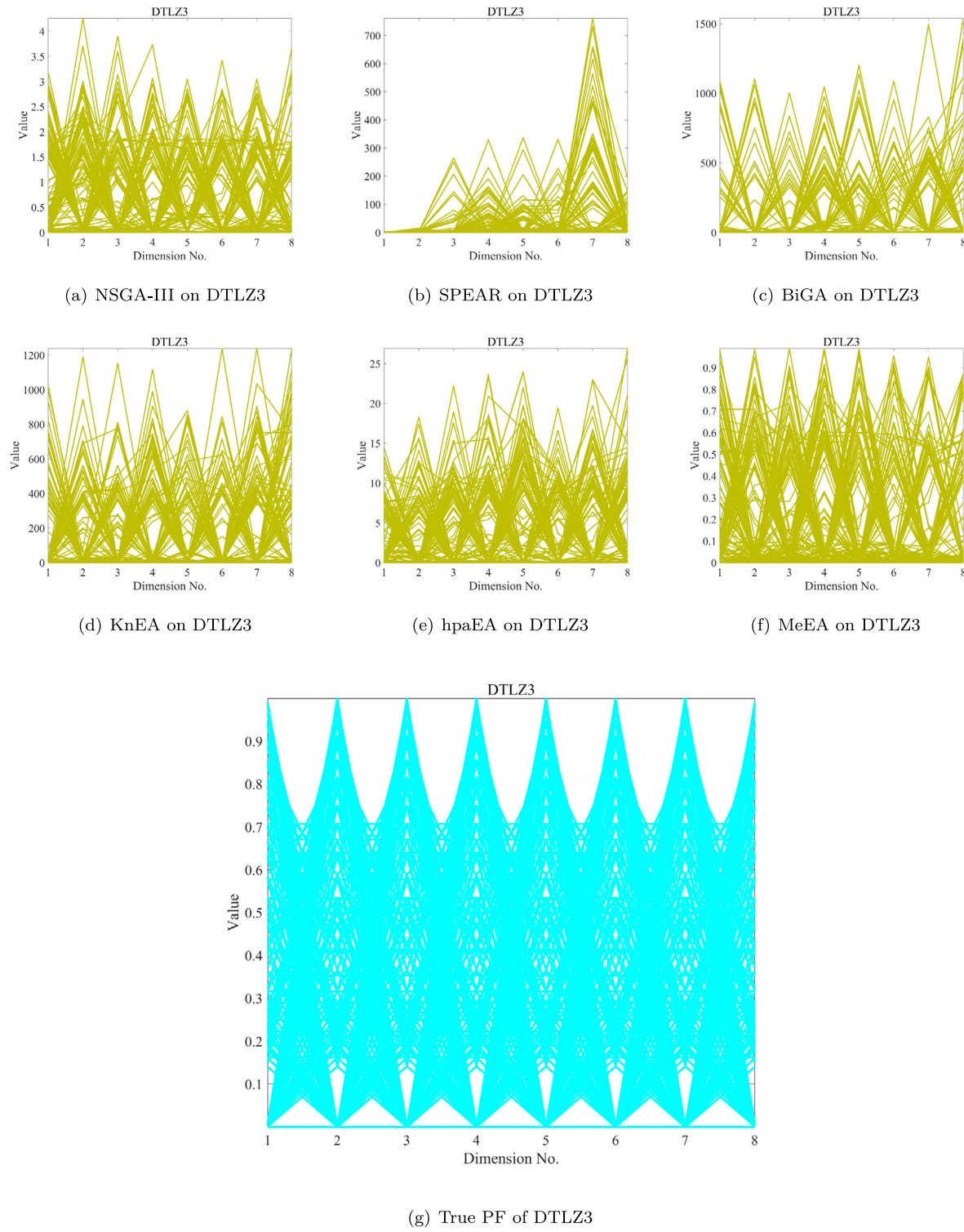


**Fig. 8.** The output populations of the six algorithms on 8-objective DTLZ3. (a) NSGA-III on DTLZ3. (b) SPEAR on DTLZ3. (c) BiGA on DTLZ3. (d) KnEA on DTLZ3. (e) hpaEA on DTLZ3. (f) MeEA on DTLZ3. (g) True PF of DTLZ3.

where  $\omega$  is the angular velocity of the journal;  $p$  is the average specific pressure of the bearing;  $\xi$  is the ratio coefficient of bearing width to diameter. When  $B/d \geq 1$ ,  $\xi = 1$ , otherwise  $\xi = (d/B)^{1.5}$ ;  $F$  is the working load of the bearing;  $v$  is the circumferential velocity of the journal.

### 5.1.3. Constraint condition

To avoid the metal contact between the raceways in the bearing and lead to bearing wear, the influence of friction surface roughness, minimum oil film thickness, elasticity and thermal deformation of shaft and bearing, cleanliness of lubricant, and size

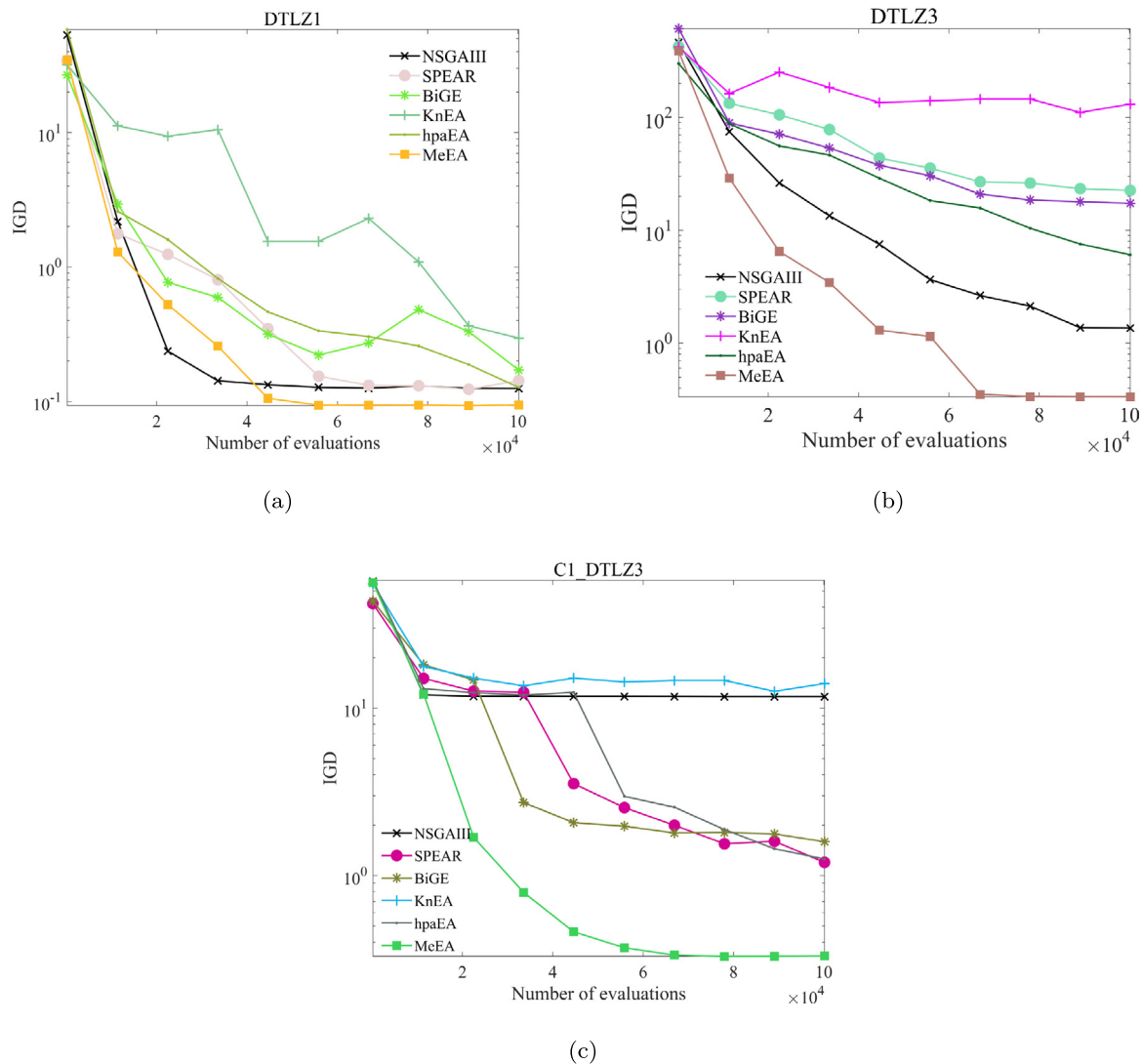


**Fig. 9.** On the 8 objective DTLZ1, DTLZ3 and C1\_DTLZ3 problems, the IGD evolution trajectory of the six algorithms.

of impurities must be considered. Therefore, the first constraint is as follows:

$$g_1(X) = k(R_{z1} + R_{z2}) - 55 \frac{nd^3 x_3 x_1^2}{F x_2 (x_1 + 1)} \leq 0 \quad (6)$$

where  $k$  is the safety factor considering geometric errors, installation errors, Journal deformation, etc., usually taken as  $k = 2 \sim 3$ ;  $R_{z1}$  and  $R_{z2}$  is the surface roughness of journal and bearing bore respectively.

The width-to-diameter ratio of the bearing shall comply with the design requirements as follows:

$$g_2(X) = x_1 - (B/d)_{\max} \leq 0 \quad (7)$$

$$g_3(X) = (B/d)_{\min} - x_1 \leq 0 \quad (8)$$

The specific pressure constraints are as follows:

$$g_4(X) = p_{\min} - \frac{F}{x_1 d^2} \leq 0 \quad (9)$$

$$g_5(X) = \frac{F}{x_1 d^2} - p_{\max} \leq 0 \quad (10)$$

Relative clearance of HLRSB affects bearing capacity, minimum oil film thickness, power consumption, and temperature rise of

bearings. Relative clearance of bearings shall meet the following constraints:

$$g_6(X) = \psi_{\min} - x_2 \leq 0 \quad (11)$$

$$g_7(X) = x_2 - \psi_{\max} \leq 0 \quad (12)$$

The viscosity of the lubricating oil shall meet the following requirements.

$$g_8(X) = \eta_{\min} - x_3 \leq 0 \quad (13)$$

$$g_9(X) = x_3 - \eta_{\max} \leq 0 \quad (14)$$

## 5.2. Implementation and application of MeEA

The proposed MeEA is applied to the optimum design of the HLRSB of the crane gearbox. The known workload is 35 KN, the diameter of the shaft is  $d = 0.1$  m and the speed is  $n = 1000$  r/min. Set the number of population to 500 and the maximum function evaluations to 500 000.

Parato curves for multi-objective optimization of HLRSB are shown in Fig. 12. The bearing coefficient needs to be maximized as far as possible in practical engineering. To solve the problem easily, the objective function of the bearing coefficient is

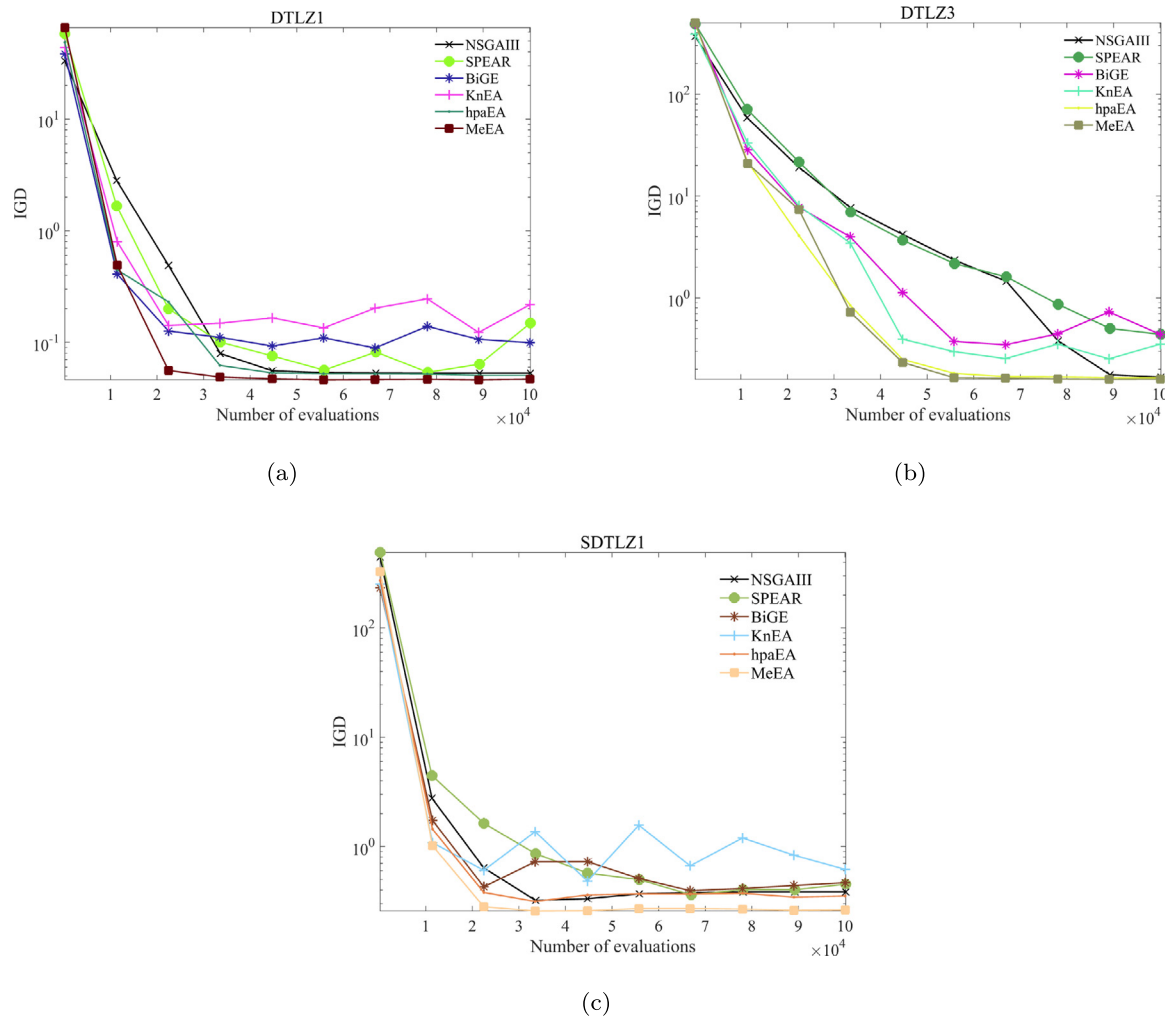


**Fig. 10.** On the 5 objective DTLZ1, DTLZ3 and SDTLZ1 problems, the IGD evolution trajectory of the six algorithms.

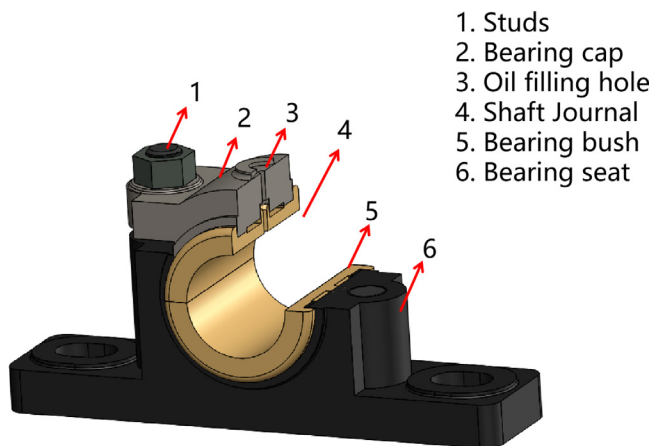


**Fig. 11.** Hydrodynamic lubrication radial sliding bearing.

converted into the minimization problem. To better observe the relationship between multiple objectives, it can be seen from Fig. 13(a) that the friction coefficient of the fluid is almost inversely proportional to the heat generated. As the friction coefficient of the fluid decreases, the heat generated increases gradually. It can be seen from Fig. 13(b) that the heat generation and the carrying coefficient are almost inversely proportional. In

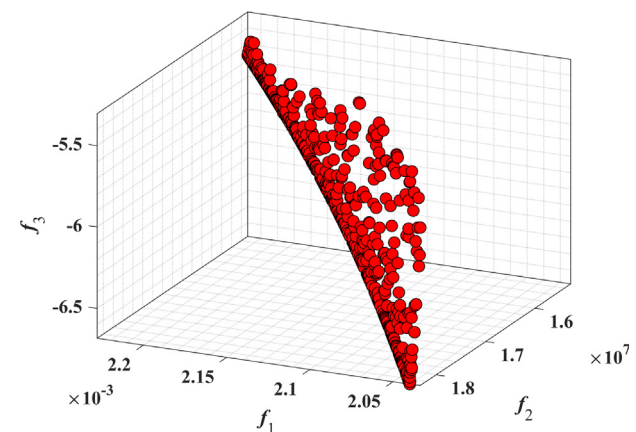
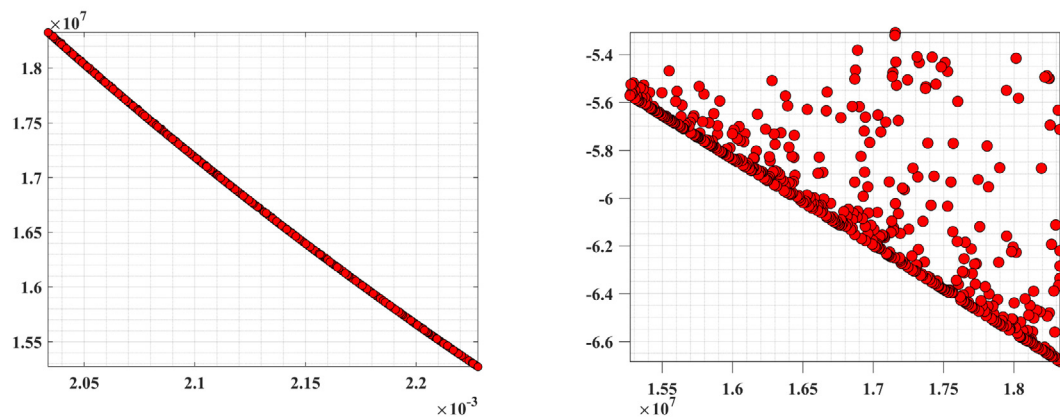


**Fig. 12.** Pareto curve for multi-objective optimization of HLRSB.

practical engineering, considering the contradictory relationship between multiple objectives, choose the appropriate position on pareto curve and select the design parameters of HLRSB according to the requirements.

In this paper, the midpoint of Fig. 12 is selected as the design parameter. From Table 6 it can be seen that the performance of optimum design using the proposed MeEA has been improved.



(a) Relationship curve between fluid friction factor and calorific value (b) Relationship curve between calorific value and load factor

**Fig. 13.** Parato curve of relationship between two objectives.

**Table 6**  
Comparison of optimization design results with conventional design results.

Design method	Design variable			Objective function		
	B/d	$\psi$	$\eta$	f	$pv$	$C_p$
Conventional design	1.0	0.001	0.018	0.0024	18.4	1.86
<b>Optimal design</b>	<b>1.08</b>	<b>0.002</b>	<b>0.02</b>	<b>0.0021</b>	<b>16.97</b>	<b>6.19</b>

Compared with the conventional design, the friction coefficient is reduced by 12.5%, heat generation is reduced by 7.7% and bearing capacity is increased by 232.7%. This optimized scheme has more practical value in engineering practice.

## 6. Conclusion

In high-dimensional space, the balance of convergence and diversity at the pareto frontier has an extremely important impact on population evolution. Due to the complexity of objective space, the local space of population distribution is sparse, crowded, and inefficient in evolution. To alleviate the contradiction between convergence and diversity, a multi-objective evolutionary algorithm with multiple ecological environment selection strategies is proposed. Firstly, the objective space is divided into multiple ecological environments with different characteristics. Secondly, multi-ecological environment selection strategy is proposed. When the number of non-dominated solutions is greater than the number of populations, preference for convergence or diversity in the ecological environment is given priority, and overall diversity maintenance is taken into account; otherwise, non-dominant solutions are preferred, and partial dominant solutions are used to maintain diversity later. Thirdly, by comparing the proposed MeEA algorithm with five popular algorithms on 44 benchmark problems, it is verified that MeEA has obvious advantages in the relationship between balance convergence and diversity. Finally, the application of this algorithm in the HLRSB of the gearbox proves that MeEA can solve practical problems well.

Future research work can be considered from two perspectives. On the one hand, the mapping between population distribution and evolutionary environment can be refined. At present, the description of multi-ecological environment to the objective space is still fuzzy and cannot fully reflect the attributes of the objective space and the impact of the objective space on population evolution. Therefore, we can study the mapping relationship between them to improve the efficiency of population evolution. On the other hand, refine the environment selection

strategy. Different objective Spaces have different characteristics, and a single evolutionary strategy still lacks self-adaptation to the evolution of the local space, so it cannot improve the search ability of the current objective space. Finally, by further improving the ability of multi-objective optimization algorithm to optimize high-dimensional objectives, to better solve practical problems.

## CRediT authorship contribution statement

**Shuzhi Gao:** Validation, Formal analysis, Investigation, Writing – review & editing. **Leiyu Yang:** Conceptualization, Methodology, Software, Writing – original draft, Visualization. **Yimin Zhang:** Supervision, Project administration, Funding acquisition.

## Declaration of competing interest

The authors declare that they have no known competing financial interests or personal relationships that could have appeared to influence the work reported in this paper.

## Data availability

No data was used for the research described in the article.

## Acknowledgments

This research was supported by the National Natural Science Foundation of China (No. 52275156), National Key R & D Program of China (No. 2019YFB2004400), Key (or General) project of Liaoning Provincial Department of Education (LJKZ0435).

## Appendix

### Nomenclature

$B/d$	Width-diameter ratio
$\psi$	Relative clearance
$\eta$	Dynamic viscosity of lubricating oil
$\omega$	Angular velocity of Journal in rad/s
$p$	Average specific pressure of bearing
$d$	Bearing diameter in m
$F$	Bearing working load in N
$v$	Circumferential velocity of Journal
$\xi$	Bearing width-diameter ratio coefficient

$k$	Safety factor for geometric shape error, installation error and journal deformation
$R_{z1}$	Surface roughness of Journal
$R_{z2}$	Surface roughness of bearing bore
$f$	Liquid friction coefficient
$p_v$	Heat generation
$C_p$	Carrying capacity coefficient

## References

- [1] Z. Wang, Y. Ong, H. Ishibuchi, On scalable multiobjective test problems with hardly dominated boundaries, *IEEE Trans. Evol. Comput.* 23 (2019) 217–231.
- [2] M. Negnevitsky, Artificial intelligence: A guide to intelligent systems, *Inf. Comput. Sci.* 48 (48) (2005) 284–300.
- [3] R. Kundu, S. Das, R. Mukherjee, S. Debchoudhury, An improved particle swarm optimizer with difference mean based perturbation, *Neurocomputing* 129 (2014) 315–333.
- [4] N.J.D. Gautier, N. Manzanares-Filho, E.R. da Silva Ramirez, Multi-objective optimization algorithm assisted by metamodels with applications in aerodynamics problems, *Appl. Soft Comput.* 117 (2022) 108409.
- [5] Z. Chen, H. Wu, Y. Chen, L. Cheng, B. qian Zhang, Patrol robot path planning in nuclear power plant using an interval multi-objective particle swarm optimization algorithm, *Appl. Soft Comput.* 116 (2022) 108192.
- [6] Y. Abdi, M.-R. Feizi-Derakhshi, Hybrid multi-objective evolutionary algorithm based on Search Manager framework for big data optimization problems, *Appl. Soft Comput.* 87 (2020) 105991.
- [7] K. Deb, S. Agrawal, A. Pratap, T. Meyarivan, A fast and elitist multiobjective genetic algorithm: NSGA-II, *IEEE Trans. Evol. Comput.* 6 (2002) 182–197.
- [8] E. Zitzler, M. Laumanns, L. Thiele, SPEA2: Improving the Strength Pareto Evolutionary Algorithm, Technical Report Gloriastrasse 3242, 2001, pp. 742–751.
- [9] A.L. Jaimes, R.V.S. Quintero, C. Coello, Ranking Methods in Many-Objective Evolutionary Algorithms, Vol. 193, Springer Berlin Heidelberg, 2009, pp. 413–434.
- [10] Liu, Xiaohui, Miqing, Yang, Shengxiang, Bi-goal evolution for many-objective optimization problems, *Artif. Intell.: Int. J.* 228 (2015) 45–65.
- [11] H. Ishibuchi, N. Tsukamoto, Y. Nojima, Evolutionary many-objective optimization: A short review, in: 2008 IEEE Congress on Evolutionary Computation (IEEE World Congress on Computational Intelligence), 2008, pp. 2419–2426.
- [12] Y. Xiang, Y. Zhou, M. Li, Z. Chen, A vector angle-based evolutionary algorithm for unconstrained many-objective optimization, *IEEE Trans. Evol. Comput.* 21 (2017) 131–152.
- [13] H.E. Aguirre, K. Tanaka, Space partitioning with adaptive ranking and substitute distance assignments: a comparative study on many-objective mnk-landscapes, in: Proceedings of the 11th Annual Conference on Genetic and Evolutionary Computation, 2009, pp. 547–554.
- [14] F. Pierro, S. Khu, D. Savic, An investigation on preference order ranking scheme for multiobjective evolutionary optimization, *IEEE Trans. Evol. Comput.* 11 (2007) 17–45.
- [15] S. Cheng, M. Chen, P. Fleming, Improved multi-objective particle swarm optimization with preference strategy for optimal DG integration into the distribution system, *Neurocomputing* 148 (2015) 23–29.
- [16] Z. He, G. Yen, J. Zhang, Fuzzy-based Pareto optimality for many-objective evolutionary algorithms, *IEEE Trans. Evol. Comput.* 18 (2014) 269–285.
- [17] M. Laumanns, R. Zenklusen, Stochastic convergence of random search methods to fixed size Pareto front approximations, *European J. Oper. Res.* 213 (2011) 414–421.
- [18] X. Zhang, Y. Tian, Y. Jin, A knee point-driven evolutionary algorithm for many-objective optimization, *IEEE Trans. Evol. Comput.* 19 (2015) 761–776.
- [19] H. Chen, Y. Tian, W. Pedrycz, G. Wu, R. Wang, L. Wang, Hyperplane assisted evolutionary algorithm for many-objective optimization problems, *IEEE Trans. Cybern.* 50 (2020) 3367–3380.
- [20] B. Qu, G. Li, L. Yan, J.J. Liang, C. Yue, K. Yu, O.D. Crisalle, A grid-guided particle swarm optimizer for multimodal multi-objective problems, *Appl. Soft Comput.* 117 (2022) 108381.
- [21] M. Li, J. Zheng, L. Ke, Q. Yuan, R. Shen, Enhancing diversity for average ranking method in evolutionary many-objective optimization, *DBLP* 6238 (2010) 647–656.
- [22] J. Bader, E. Zitzler, HypE: An algorithm for fast hypervolume-based many-objective optimization, *Evol. Comput.* 19 (2011) 45–76.
- [23] K. Shang, H. Ishibuchi, L. He, L.M. Pang, A survey on the hypervolume indicator in evolutionary multiobjective optimization, *IEEE Trans. Evol. Comput.* 25 (2021) 1–20.
- [24] K. Li, K. Deb, Q. Zhang, S. Kwong, Combining dominance and decomposition in evolutionary many-objective optimization, *IEEE Trans. Evol. Comput.* (2014) 1.
- [25] M. Li, S. Yang, X. Liu, Pareto or non-Pareto: Bi-criterion evolution in multiobjective optimization, *IEEE Trans. Evol. Comput.* 20 (2016) 645–665.
- [26] S. Lin, F. Lin, H. Chen, W. Zeng, A MOEA/D-based multi-objective optimization algorithm for remote medical, *Neurocomputing* 220 (2017) 5–16.
- [27] Y. Hu, J. Wang, J. Liang, Y. Wang, U. Ashraf, C. Yue, K. Yu, A two-archive model based evolutionary algorithm for multimodal multi-objective optimization problems, *Appl. Soft Comput.* 119 (2022) 108606.
- [28] P. Wang, X. Tong, A dimension convergence-based evolutionary algorithm for many-objective optimization problems, *IEEE Access* 8 (2020) 224631–224642.
- [29] C. He, Y. Tian, Y. Jin, X. Zhang, L. Pan, A radial space division based evolutionary algorithm for many-objective optimization, *Appl. Soft Comput.* 61 (2017) 603–621.
- [30] K. Deb, H. Jain, An evolutionary many-objective optimization algorithm using reference-point-based nondominated sorting approach, Part I: Solving problems with box constraints, *IEEE Trans. Evol. Comput.* 18 (2014) 577–601.
- [31] C. Wang, H. Pan, Y. Su, A many-objective evolutionary algorithm with diversity-first based environmental selection, *Swarm Evol. Comput.* 53 (2020) 100641.
- [32] H. Ge, M. Zhao, L. Sun, Z. Wang, G. Tan, Q. Zhang, C. Chen, A many-objective evolutionary algorithm with two interacting processes: Cascade clustering and reference point incremental learning, *IEEE Trans. Evol. Comput.* 23 (2019) 572–586.
- [33] M. Li, S. Yang, X. Liu, A performance comparison indicator for Pareto front approximations in many-objective optimization, in: ACM, 2015, pp. 703–710.
- [34] W. Qiu, J. Zhu, G. Wu, M. Fan, P. Suganthan, Evolutionary many-objective algorithm based on fractional dominance relation and improved objective space decomposition strategy, *Swarm Evol. Comput.* 60 (2021) 100776.
- [35] S. Jiang, S. Yang, A strength Pareto evolutionary algorithm based on reference direction for multiobjective and many-objective optimization, *IEEE Trans. Evol. Comput.* 21 (2017) 329–346.
- [36] Y. Tian, R. Cheng, X. Zhang, Y. Jin, PlatEMO: A MATLAB platform for evolutionary multi-objective optimization [Educational Forum], *IEEE Comput. Intell. Mag.* 12 (2017) 73–87.
- [37] K. Deb, L. Thiele, M. Laumanns, E. Zitzler, Scalable test problems for evolutionary multi-objective optimization, *Evol. Multiobj. Optim.* (2006) 105–145.
- [38] Fellow, IEEE, H. Jain, K. Deb, An evolutionary many-objective optimization algorithm using reference-point based nondominated sorting approach, Part II: Handling constraints and extending to an adaptive approach, *IEEE Trans. Evol. Comput.* 18 (4) (2014) 602–622.
- [39] P. Bosman, D. Thierens, The balance between proximity and diversity in multiobjective evolutionary algorithms, *IEEE Trans. Evol. Comput.* 7 (2003) 174–188.
- [40] E. Zitzler, L. Thiele, Multiobjective evolutionary algorithms: a comparative case study and the strength Pareto approach, *IEEE Trans. Evol. Comput.* 3 (1999) 257–271.
- [41] H. Ishibuchi, R. Imada, Y. Setoguchi, Y. Nojima, Reference point specification in hypervolume calculation for fair comparison and efficient search, in: Proceedings of the Genetic and Evolutionary Computation Conference, 2017, pp. 585–592.
- [42] Z. Yi, X. Zheng, X. Wan, D. Zhang, Optimization design of hydrodynamic sliding bearing based on differential cellular genetic algorithm, *J. Mech. Transm. (38)* (2014) 64–68.
- [43] W. Hou, S.O. Aerocraft, X.A. University, Hybrid multi-objective optimization for hydrodynamic bearing design, *Control Eng. China* 25 (2018) 1044–1049.